

DESIGN OF FOUR ELEMENT PATCH ARRAY ANTENNA
FOR IEEE 802.11 AT 2.4 GHZ

by

Jagadish Khanal

A thesis submitted to the Graduate Council of
Texas State University in partial fulfillment
of the requirements for the degree of
Master of Science
with a Major in Engineering
May 2019

Committee Members:

Harold Stern, Chair

Karl D Stephan, Co-chair

Rich Compeau

Bill Stapleton

COPYRIGHT

by

Jagadish Khanal

2019

FAIR USE AND AUTHOR'S PERMISSION STATEMENT

Fair Use

This work is protected by the Copyright Laws of the United States (Public Law 94-553, section 107). Consistent with fair use as defined in the Copyright Laws, brief quotations from this material are allowed with proper acknowledgement. Use of this material for financial gain without the author's express written permission is not allowed.

Duplication Permission

As the copyright holder of this work I, Jagadish Khanal, authorize duplication of this work, in whole or in part, for educational or scholarly purposes only.

ACKNOWLEDGEMENTS

I am very fortunate for having a chance to work under my supervisor Dr. Harold Stern. Without his support and guidance this thesis would not have been possible. I feel grateful to my thesis committee members Dr. Karl D Stephan, Dr. Rich Compeau and Dr. Bill Stapleton, who gave me the opportunity to explore from their wisdom. I am really grateful for their generous support for the successful completion of my thesis.

Finally, I would like to thank my family and friends for their motivation and encouragement throughout my life.

TABLE OF CONTENTS

	Page
ACKNOWLEDGEMENTS	iv
LIST OF TABLES	vii
LIST OF FIGURES	viii
ABSTRACT	x
CHAPTER	
1. INTRODUCTION	1
1.1 History of Wireless Communication via Electromagnetic Waves	1
1.2 History of the Microstrip Patch Antenna and its compatibility with IEEE 802.11 protocol	2
1.3 Microwave Frequencies in Wireless Communication	5
2. BASICS OF ANTENNAS	6
2.1 Fundamental Principles of Antennas	6
2.2 Radiation Pattern	7
2.3 Near and Far-Field Regions	8
2.4 Radiation Power Density and Radiation Intensity	10
2.5 Directivity and Gain	10
2.6 Polarization	12
2.7 Antenna Bandwidth (BW)	14
2.8 Frequency Scaling	15
3. INTRODUCTION TO MICROSTRIP PATCH ANTENNA	17
3.1 Modeling of Rectangular-Microstrip Antenna	21
3.1.1 Transmission Line Model	21
3.1.2 Cavity Model	24
4. ARRAY ANTENNA	27
4.1 Linear Array Factor	28
4.2 Planar Array Factor	29

5. COMPUTER PROGRAM FOR SIMULATION OF HIGH FREQUENCY DEVICES.....	32
5.1 Create model/Geometry	33
5.2 Assign Boundary.....	33
5.3 Excitation in HFSS	34
5.4 Solution Frequency	35
5.5 The Delta S	36
5.6 Post Processing	36
6. DESIGN AND SIMULATION OF SINGLE ELEMENT RECTANGULR PATCH ANTENNA	38
7. FOUR ELEMENT ARRAY OF RECTANGULAR MICROSTRIP PATCH	46
8. SCUSSION, CONCLUSION AND SUGGESTION FOR FUTURE RESEARCH	54
8.1 Discussion and Conclusion	54
8.2 Suggestion for Future Research.....	57
8.2.1 Single Element R-MPA	57
8.2.2 Transmission line	58
REFERENCES	59

LIST OF TABLES

Table	Page
1.1 Different IEEE 802.11 standards year adopted, frequency, speed and notes	3
1.2 Bandwidth allocation for different channels for IEEE 802.11b standards	4
3.1 List of common suitable substrates for MPA	18
8.1 Summary of targeted, simulated and measured antenna parameters	57

LIST OF FIGURES

Figure	Page
3.1 Rectangular Microstrip Patch Antenna	19
3.2 Electric field lines in a microstrip line generating effective dielectric constant	21
3.3 Inset feed to 50Ω region of patch.....	23
3.4 Cavity model representation of R-MPA	24
3.5 Effect of fringing field in R-MPA	25
4.1 Representation of planar array	29
4.2 Simulated rectangular array	31
6.1 Top view of R-MPA	39
6.2 Simulated (red) and measured (blue) S11.....	41
6.3 Polar plot of realized gain in 2-D.....	42
6.4 Polar plot of directivity of R-MPA in 3-D.....	43
6.5 Surface current gradient under the patch	44
7.1 ‘4×1’ Power splitter using microstrip line	46
7.2 S11, S21, S31, S41 and S51 of the ‘4×1’ power splitter	47
7.3 Array antenna being measured in anechoic chamber	48
7.4 Simulated (red) and measured (blue) S11.....	49
7.5 Gain vs frequency plot	50
7.6 Simulated 2-D plot of realized gain of the array antenna	51
7.7 Measured 2-D plot of realized gain in dB of the array antenna.....	51

7.8 Simulated Directivity of the array antenna in 3D	52
7.9 Measured directivity of the array antenna (2D).....	53
7.10 Measured efficiency of the array antenna.....	53
8.1 Four element array antenna (220 mm × 225 mm board size).....	55

ABSTRACT

This is a very exciting time to investigate microstrip (aka. patch or printed) antennas because the world of technology is ready to take a big step towards the Internet of Things (IOT). With IOT almost every device we are involved with will communicate with one another. The only reasonable medium for communication will be wireless communication. Wireless communication involves antennas and antenna design always involves topics like size, flexibility, power consumption, efficiency, cost and weight.

Out of the myriad list of antennas present in today's world, microstrip antennas are among the most promising when it comes to ease of fabrication and extremely low profiles. They can hide under circuit boards, they can be made super flexible and very light. It is a wise assumption that almost all IOT devices will employ a printed antenna.

In this thesis design, simulation, optimization, fabrication and characterization of a rectangular patch antenna has been done. The designed antenna was compatible with the IEEE 802.11b protocol for Wi-Fi as it was resonating at 2.4 GHz and the other antenna parameters like bandwidth, gain and Half Power Beam Width (HPBW) were also suitable for the protocol. This antenna was then used to design a four element patch array antenna. The performance of the array antenna was then compared with respect to the initially designed single rectangular patch antenna. After characterizing the array antenna in an anechoic chamber it was found that the array antenna has a gain of 12.5 dB which is 5.21 dB higher than the simulated gain of the initially designed single element antenna. The

array antenna has a frequency bandwidth of 70 MHz and an efficiency of 80%. Both single element antenna and the array antenna can be used as a radiating element for IEEE 802.11b protocol. However, out of fourteen channels defined under the protocol, the single element antenna can fully support only up to channel number eight and partially support channel number nine. The array can fully support up to channel number ten and partially support channel number eleven.

1. INTRODUCTION

1.1 History of Wireless Communication via Electromagnetic Waves

The discovery of electromagnetism is often credited to Hans Oersted in 1819 for observing that the needle of a magnetic compass can be deflected using a current-carrying wire. Soon in 1840, Joseph Henry observed high-frequency electric oscillations at a distance from their source. Such electromagnetic waves were then mathematically described in 1861 by James Maxwell and presented in theory at the Royal Society of London in Dec 1864, later published in 1873.

While contributions by Heinrich Rudolph Hertz and other prestigious scientists like Sir Oliver Lodge, Augusto Righi, Popov, Lebedew, Pampa, and others cannot be overlooked, the demonstration by Guglielmo Marconi in 1896 is considered the paramount event in the field of wireless communication. Marconi installed a 1.7 mile, radio telegraph system for the British Post Office. The following year, Marconi installed the first permanent wireless station on the Isle of Wight and communicated with ships. The next year he added a second station at Bournemouth. This system is described by George Kizer as the first permanent point-to-point wireless link in his book in 2013[1].

Overall, the late 19th to the mid 20th century has been a hallmark of wireless communication. In this era, myriads of inventions were deployed. A few of the key innovations are listed below:

1894: Coaxial cable, patented by Nikola Tesla in the USA

1897: Cathode Ray Tube with a magnetic deflection and CRT oscillator by

Karl Ferdinand Braun

1909: Theoretical Integral Equation solution to free space radio wave propagation by Arnold Sommerfeld

1914: AM Modulator circuit by Edwin H. Colpitts

1918: Superheterodyne receive by Edwin H. Armstrong

1930: Radio Detection and Ranging (RADAR) developed simultaneously by several countries

1935: 3 GHz multi-cavity Magnetron by Hans Hollmann

1936: Frequency Modulation by Edwin H. Armstrong

1937: Klystron Oscillator by Sigurd and Rossell

1944: N-connectors like BNC, TNC, SMA by Paul Neill at Bell Labs

1950: stripline and Micro-strip printed circuit technology

1961: Gallium-Arsenide (GaAs) semiconductors by Biard and Pittman at Texas Instrument

1.2 History of the Microstrip Patch Antenna and its compatibility with IEEE 802.11 protocol

Though first introduced in 1953 and patented in 1955, the fame of the microstrip patch antenna (MPA) was mostly limited to theory until printed circuit board (PCB) technology was introduced in 1970[2, 3]. After the popularity of PCB technology, MPA became the first choice for most wireless communication devices like cell phones, GPS, RFID and satellites. This is due to its promising features like low weight and profile, low cost, easy conformability and portability, easy fabrication and easy integration to other electronic

circuitry, despite the fact that the patch antenna suffers major problems of very narrow bandwidth and low gain.

Fortunately, the IEEE 802.11 protocol requires very narrow bandwidth to operate, which makes MPA a good match for the system. Generally, the resonant frequency and the range of bandwidth required is dependent on different subsections of the protocol and is also governed by the country where the associated device is to be operated. Some different standards in 802.11 protocol with their operating frequency and other information is tabulated below.

Table 1.1 Different IEEE 802.11 standards year adopted, frequency, speed and notes [4]

IEEE Standards	Speed	Frequency	Notes
802.11	1 Mbps, 2 Mbps	2.4 GHz	FirstPHY standard (1997)
802.11 a	Up to 54 Mbps	5 GHz	SecondPHY standard (1999)
802.11 b	55 Mbps, 11 Mbps	2.4 GHz	ThirdPHY standard
802.11 g	Up to 54 Mbps	2.4 GHz	FourthPHY standard (2003)
802.11 n	Up to 288 Mbps (20 MHz channel), Up to 600 Mbps (40 MHz channel)	2.4 GHz, 5GHz	Launched in 2009

Since this thesis focuses on development of a patch antenna at 2.4 GHz, 802.11 (b, g, n, af, ah and ax) can be potential candidates for the proposed antenna.

The IEEE 802.11 protocol has 14 different channels. Channel 1 has a central frequency at 2.412 GHz and channel 14 has central frequency at 2.484 GHz[5]. Thus an antenna with bandwidth of 100 MHz with lower frequency of 2.4 GHZ and upper frequency of 2.5 GHz

can serve as an excellent radiator for 802.11 standards at 2.4 GHz [5].

Table 1.2 Bandwidth allocation for different channels for IEEE 802.11b standards

CHANNEL NUMBER	LOWER FREQUENCY MHZ	CENTER FREQUENCY MHZ	UPPER FREQUENCY MHZ
1	2401	2412	2423
2	2406	2417	2428
3	2411	2422	2433
4	2416	2427	2438
5	2421	2432	2443
6	2426	2437	2448
7	2431	2442	2453
8	2436	2447	2458
9	2441	2452	2463
10	2446	2457	2468
11	2451	2462	2473
12	2456	2467	2478
13	2461	2472	2483
14	2473	2484	2495

This thesis focuses on design, fabrication and testing of an MPA that can support the IEEE 802.11b protocol. Studies on several aspects of the antenna such as substrates, impedance, bandwidth, scattering parameter and radiation characteristic for the antenna have been performed and are presented in detail in chapters to come. Chapter two provides a short discussion of antenna basics and explains why certain performance targets were chosen for the MPA. Chapter three describes properties of MPAs and how MPAs are modeled. Chapter four provides a short introduction in the basics of array antenna. Chapter five describes simulation tools for evaluating antenna design. Chapters six and seven describe the design and simulation of the single element MPA and the design, simulation and the physical testing of the four element array MPA. Chapter eight provides conclusions and suggestions for future research.

1.3 Microwave Frequencies in Wireless Communication

The microwave frequency band ranges from 300 MHz (100 cm) to 300 GHz (0.1 cm), which is in fact a small part of the band of radio wave frequencies, which range from 3 KHz (100 km) to 300 GHz. This 300 MHz to 300 GHz range of frequencies, termed as microwave, is further divided by IEEE radar terminology into S, C, X, Ku, K, Ka bands. Similar subdivisions can also be found by other designators like NATO and EU. Out of the entire microwave band, the most used frequencies for communication are within the approximate range of 2 to 38 GHz [6]. The general sharing of the available band between several users like telecom, radio, military, avionics, satellite etc. is organized by the International Telecommunication Union-Radiocommunication (ITU-R) sector. ITU-R also governs other factors like maximum power or EIRP, restricted radiation antenna pattern, restricted spurious and out-of-band signals, geographical site exclusion, time cycle use, channel spacing and capacity. A general list of frequency band and channel capacity for digital microwave radio systems is given in [7].

2. BASICS OF ANTENNAS

2.1 Fundamental Principles of Antennas

An accelerating charge creates a disturbance in space that spreads as a time varying electric and magnetic field, collectively called an electromagnetic wave [8]. Such charge can be accelerated on a wire, which will then be called a wired antenna. Such wired antennas can be properly shaped to improve the radiation characteristics. For example, a dipole is a pair of wire antennas. A helical antenna is a twisted wire. A bunch of wires (or dipoles) are used in a log-periodic antenna. Equation (2.1) describes the general idea that to create radiation, there must be a time-varying current or an acceleration (or deceleration) of charge. To create this effect a wire can be bent, curved or terminated.

$$L \frac{dI}{dt} = Lq \frac{dv}{dt} = L \times q \times a \dots (2.1)$$

Here, ‘L’ is the length of wire, ‘q’ is the charge and ‘a’ is the acceleration.

In a broad sense, a section of such wires, all of them radiating individually, if designed and arranged properly, will constructively interfere in the area of interest, thereby increasing radiation efficiency in the desired direction. But in other directions, the energy is substantially reduced, also explained by the law of conservation of energy. For this reason, isotropic antennas don’t exist in reality but they are still used mathematically for comparison purposes to all other antennas.

There are various fundamental parameters that can be considered when studying any antenna.

The gravity of such parameters depends on the nature of antenna being designed. Some of the basic and commonly used properties are briefly discussed below. Later, these terms will be used in describing the microstrip patch antenna designed for this thesis.

2.2 Radiation Pattern

A radiation pattern is defined as “*a mathematical function of a graphical representation of the radiation properties of the antenna as a function of space coordinates [8].*” A trace of received electric or magnetic field at a constant radius is called an amplitude field pattern. A similar graph which has power flux is called an amplitude power pattern. Most of the time, the magnitudes are normalized to a decibel scale so that the low power and high power components of the signal can be contrasted together in a single graph.

The graph that represents radiation pattern can also be used to identify major lobes and minor lobes. The minor lobes include the side and the back lobe. The major lobe is the portion that carries a significant amount of energy. It gives the sense of where the bore sight is (the axis along which the most useful amount of power is directed). The graph also illustrates several frequently used parameters, like the front to back ratio, the half power beam width (HPBW), the first null beam width and the half null beam width. An antenna like the one used in Wi-Fi-routers might want a large HPBW so that it can cover an entire floor and minimize the complexity of having multiple antennas. Likewise, some antennas like the ones used in satellites might require a highly focused beam so that the information-carrying wave can penetrate longer distances with less loss.

The targeted half power beam width of the single element MPA designed in this thesis is 80-100 degrees. This target was chosen because for this angle Wi-Fi routers are most likely

to cover major portions of the floors even without energy reflecting from the surrounding walls.

2.3 Near and Far-Field Regions

A micro-strip antenna is a conductive metal coating fabricated on a substrate (i.e. dielectric) which has a conducting ground plane on one side, making it a parallel plate capacitor. Materials like silver, copper, aluminum etc. that are used for fabricating antennas have inherit parasitic reactance with them [9]. The effect of such parasitic reactance is frequency-dependent and generally increases with increasing frequency.

The capacitance and inductance nature of an antenna is responsible for storing energy in the form of electric (E) and magnetic (H) fields in its vicinity. This energy is not directly radiated, but any kind of influence on this area can drastically disturb the performance of the antenna.

To properly study the sensitive areas near an antenna, the area around it is generally classified into three regions. Though the regions are described by separate equations, it should be kept in mind that the region-classification may not always be realistic for all antennas, and further analysis may be required. Generally, the regions around the antenna are distinguished as the reactive near field, the radiating near field and the far-field.

The region around an antenna where the reactive field predominates is called the reactive near-field region and its radius is $R < 0.62 D^3/\lambda$ where λ is the wavelength at which the antenna operates and D is the largest dimension for that antenna.

The region that follows the reactive near-field is called the radiating near-field (Fresnel) region. In this region the angular field distribution depends on the distance from antenna. Generally, this region is defined as: $0.62 D^3\lambda < R < 2D^2\lambda$. The space that follows the Fresnel region is called the far-field (Fraunhofer) region and is identified as space whose radius is greater than $2D^2\lambda$. The characteristics of the antenna in the far-field allow it to be considered as an electric dipole where the magnitude of the electric field and the magnitude of the magnetic field follow the inverse square law. Thus, the far-field can exist far from the antenna. The far-field can also be recognized as the region where the wave pattern is uniform, i.e. the wave can be considered as a plane wave. Here, the time varying electric field is responsible for generation of the magnetic field and in turn this magnetic field helps generate the electric field. These E and H field vectors are 90 degrees apart from one another and the direction of propagation is given by the cross product of the two vectors [10].

Near-field can be considered as a multipole whose field decay follows a combination of inverse square and inverse cubical law. Thus, such a field vanishes within a few λ away. In the near field, electric and magnetic fields can exist independently. Some antennas can reliably operate, or in another term, can wirelessly communicate, using near-field radiation only. The near-field is also used in capacitive-sensing techniques. Such techniques are used to study the impact of objects like the human body near the antenna. The near-field of the antenna inside many smart watches (for example, Apple-watch) is always accompanied by a human wrist, and thus the capacitive nature of the human body is considered when designing antennas for such a watch.

2.4 Radiation Power Density and Radiation Intensity

The electromagnetic energy radiating from any antenna carries a certain power with it. To quantify the power associated with an antenna, the instantaneous Poynting vector is introduced.

$$W = E \times H \dots (2.2)$$

where E and H are the magnitude of the electric and magnetic field respectively.

The total power flux (P) passing through an entire surface is the surface integral of this quantity:

$$P = \iint W \cdot ds \dots (2.3)$$

P can also be derived as [8]

$$P = 0.5 \times \iint Re(E \times H) \cdot ds \dots (2.4)$$

Radiation intensity (U) in a given direction is the power radiated from an antenna per unit solid angle. This is a far-field parameter which can be obtained by multiplying radiation density by the square of the distance:

$$U = r^2 \times W \dots (2.5)$$

2.5 Directivity and Gain

According to the International Electrotechnical Commission (IEC), directivity of an antenna is defined as “the ratio of the radiation intensity in a given direction from the antenna to the radiation intensity averaged over all directions. The average radiation intensity is equal to the total power radiated by the antenna divided by 4π . If the direction is not specified, the direction of maximum radiation intensity is implied.”

Mathematically,

$$\text{Directivity (D)} = \frac{U}{U_0} = \frac{4\pi U}{P} \dots (2.6)$$

Directivity can also be expressed as

$$D = \frac{P}{P_{avg}} \dots (2.7)$$

where P is power density at its maximum point and P_{avg} is average power density.

Because directivity is solely based on the shape of the radiative pattern of the antenna and it doesn't account for the losses that may actually occur in a real antenna system, a term called Gain (G) is introduced. Gain is given by

$$G = k \times D = k \frac{P}{P_{avg}} \dots (2.8)$$

where k = efficiency (i.e. power radiated divided by power input) of the antenna. Efficiency will be discussed briefly later in this thesis.

Thus, for most of antennas whose efficiency is very high, gain is almost equal to directivity[11]. Generally, the sharper the lobe, the more the gain of the antenna will be. For cases where side lobes are comparatively smaller than the main lobe, the following approximation can be used [8]:

$$G \approx \frac{41253}{H_{3dB} \times E_{3dB}} \dots (2.9)$$

The overall gain for an antenna also depends on the transmission line that connects the power source to the antenna. Such a transmission line has a different characteristic impedance than the antenna in general, which results in reflection of some signal. Such reflection generates reflection loss (also known as mismatch loss). This loss is taken into account by introducing reflection efficiency

$$\text{reflection efficiency (e}_r\text{)} = 1 - \text{mag}(\Gamma)^2 \dots (2.10)$$

where Γ is the reflection coefficient, defined as

$$\Gamma = \frac{Z_{in} - Z_0}{Z_{in} + Z_0} \dots (2.11)$$

Here, Z_{in} and Z_0 are the impedance of the antenna and the transmission line. Thus, realized gain $G_{re} = G \times e_r \dots (2.12)$

The targeted gain of the single element MPA designed in the thesis is around 7 dBi. This target was chosen based on several literature reviews [8] on possible maximum gain of a RMPA.

2.6 Polarization

Polarization is a crucial characteristic of an antenna. Mismatch in polarization can cause significant power loss. For most of the cases, the far-end and near-end antennas must have the same degree and type of polarization.

The electric field plays a vital role in defining the polarization of any EM field. Polarization of a radiated wave is defined as “that property of electromagnetic wave describing the time varying direction and relative magnitude of electric field vector; specifically, the figure traced as a function of time by the extremity of the vector at the fixed location in space, and the sense in which it is tracked, as observed along the direction of propagation [11].” Generally used polarizations in antennas are linear polarization (vertical and horizontal) and elliptical polarization.

In linear polarization, the E field is always pointing in the same direction (expect for a sign change). And its counterpart, the H field is 90 degrees apart from the E field. If the E field (or vector) is parallel to the Earth’s surface it is then termed a horizontally polarized wave (or antenna). Similarly, if the E-vector is perpendicular to the Earth’s surface, then it is called a vertically polarized wave or vertically polarized antenna. The time phase

difference between two components of a linearly polarized wave must be equal to $n\pi$, where $n=1,2,3\dots$

Elliptical polarization is achieved only when the time phase difference between two components is an odd multiple of $\pi/2$. In such a case, if magnitude of two components (i.e. E and H) is the same then it is a special case of elliptical polarization called circular polarization; otherwise, it is simply elliptical polarization. Circular polarization is frequently used for space communication. If vertical and horizontal elements in the same plane are fed out of phase, the resultant polarization is elliptical polarization[8].

In practice, in the case of some antennas, the rectangular opening at the end of a rectangular wave guide can be used to excite an antenna either horizontally or vertically. If the smaller breadth of the opening is assigned perpendicular to Earth's surface, it will than make the antenna vertically polarized. Likewise, if assigned horizontally, it will make the antenna horizontally polarized. Another way to convert the polarization of an antenna is to entirely tilt the whole system (antenna and attached wave guide) by 90 degrees. A combination of antenna elements are fed out of phase in order to obtain elliptical polarization.

Mismatch in polarization generates a loss in antenna systems called the polarization loss factor (PLF). If ψ_p is the angle between two unit vectors representing the E field of the transmitter and the receiver antenna, then

$$\text{PLF} = \text{mag}(\cos \psi_p)^2 \dots (2.13)$$

This in turn give rise to another factor called polarization efficiency (P_e), which is defined as the ratio of the power received by an antenna from a given plane wave of arbitrary polarization to the power that would be received by the same antenna from a plane wave of the same power flux density and direction of propagation, whose state of

polarization has been adjusted for a maximum received power. This is similar to the PLF and it is expressed as

$$P_e = \frac{mag(le \times Einc)^2}{mag(le)^2 \times mag(Einc)^2} \dots (2.14)$$

where “le” is the vector effective length of antenna and “Einc” is incident E-field.

Linear polarization is chosen for the single element MPA designed in this thesis because most of the commercial antenna available for the 802.11b are linear. Circular polarization is helpful in cases where both receiver and transmitter are in motion, which is less likely for Wi-Fi and Bluetooth users.

2.7 Antenna Bandwidth (BW)

The range of frequency spectrum over which an antenna can show a specified level of performance is called the bandwidth of the antenna. The unit of measurement is frequency (kHz, MHz etc.) or a percentage of the antenna’s design frequency. Numerically,

$$BW = f_{max} - f_{min} \dots (2.15)$$

where f_{max} and f_{min} are the maximum and minimum frequency at which the antenna can show performances within a given specification. A common example of such a specification is 2:1 SWR bandwidth, for which f_{max} and f_{min} are, respectively, the minimum and maximum frequency for which a particular antenna has a standing wave ratio of 2:1 or less.

The percentage bandwidth of any antenna decreases if the frequency of operation is reduced. Therefore, for antennas operating at lower frequency, optimizing such antennas so that they can support larger bandwidth is a big challenge.

The targeted bandwidth of the single element MPA designed in this thesis is 73 MHz. This target was chosen because literature [8] suggests that microstrip feed MPA can only have up to 3 percent bandwidth. Thus, at 2.4 GHz the 3 percent range, which is 73 MHz, can successfully accompany up to channel 11 of the 802.11b protocol. In this case the antenna can support at least three non-overlapping channels.

2.8 Frequency Scaling

Frequency scaling is a technique whereby any physical dimension of an antenna's design can be altered (increased or decreased) so that the operating frequency of the antenna can be altered. This technique reduces the need for new designs every time the desired operating frequency is changed. The following equation can be used to model or scale any antenna:

$$D = \frac{f_1}{f_2} \times d \dots (2.16)$$

where 'f1' and 'f2' are original and scaled frequency, 'd' is the original design dimension and 'D' is scaled dimension [11].

Along with frequency scaling, one must also consider diameter scaling since the elements of antenna are 3D and not 2D. Sometimes frequency scaling yields unrealistic dimensions. In such cases, an entirely new design is preferred.

There are numerous other parameters of antennas like beam efficiency, scattering parameters, reflection and transmission coefficients, input impedance, effective length and area, temperature dependence, and so on. Though each of them play a vital role, depending on nature and necessity of design, some parameters carry huge importance while some are less significant.

For example, an antenna designer focusing on “less energy consumption” may not seriously look into areas like effective length, but might concentrate more on reflection coefficients and temperature dependence. Similarly, a designer working on flexible antennas might be interested in shift on S11 of antenna rather than polarization.

The antenna designed for this thesis is the Rectangular-MPA (R-MPA) and a four element array of the same R-MPA. The areas of interest for such antennas can be the radiation characteristics, gain, directivity and voltage standing wave ratio (VSWR). Effect of temperature, despite having some impact, may be neglected throughout the research.

3. INTRODUCTION TO MICROSTRIP PATCH ANTENNA

The rapid growth of printed circuit technology has enabled the convenience of printed antennas such as the microstrip or patch antenna in wireless devices where size, weight, low profile, and cost are extremely significant. Despite having some disadvantages like poor bandwidth, high Q and poor polarization purity, the convenience such antennas provide in terms of size, ease of fabrication, flexibility (in terms of several antenna parameters) and manufacturing cost are so attractive that copious amounts of research and investigations have been carried out on the patch antenna to improve and enhance its characteristics.

Specially, with the twenty-first century heading towards Internet of Things (IOT) where all electronics and even non-electronic devices are gradually being interconnected via wireless communication, this is also a perfect time to study any antenna which can have promising features in terms of power consumption, size and manufacturing cost.

In general, an MPA consists of three major parts - the metallic patch, the dielectric, and the ground plane. The metallic patch (of thickness $t \ll \lambda_0$) is a fraction of a wavelength ($0.003 \lambda_0 \leq h \leq 0.05 \lambda_0$) above the ground plane. The space between the patch and the ground is generally filled with a substrate of dielectric constant between 2.2 and 12. [8] Some commercially available substrates for patch antennae, along with key specifications, are listed in Table 3.1.

Table 3.1 List of common suitable substrates for MPA[8]

Company	Substrate	Thickness (mm)	Frequency (GHz)	ϵ_r	$\tan\delta$
Rogers Corporation	Duroid® 5880	0.127	0 – 40	2.20	0.0009
	RO 3003	1.575	0 – 40	3.00	0.0010
	RO 3010	3.175	0 – 10	10.2	0.0022
	RO 4350	0.168	0 – 10	3.48	0.0037
		0.508			
— DuPont Isola Arlon Polyflon Neltec Taconic		1.524			
	FR4	0.05 – 100	0.001	4.70	—
	HK 04J	0.025	0.001	3.50	0.005
	IS 410	0.05 – 3.2	0.1	5.40	0.035
	DiClad 870	0.091	0 – 10	2.33	0.0013
	Polyguide	0.102	0 – 10	2.32	0.0005
	NH 9320	3.175	0 – 10	3.20	0.0024
	RF-60A	0.102	0 – 10	6.15	0.0038

It should be noted that a thick substrate with lower dielectric constant provides better efficiency and larger bandwidth as the fields are loosely bound for radiation into space. But such a specification results in a larger electrical element size of the antenna. A thin substrate with a higher dielectric constant is desired for microwave circuitry because it requires tightly bound fields to minimize undesired radiation and coupling and leads to smaller element size [8]. This concept has been thoroughly studied and mentioned in the mathematical modelling section 3.1.2 (Cavity Model section) of this thesis. Therefore, a careful selection of substrate and thickness of the substrate has to be done so that the desired performance of the antenna is received.

The dielectric constant of a substrate affects the wavelength of the electromagnetic wave in that substrate, and since the length of the patch is directly influenced by wavelength, choosing the right substrate is very important, as it decides the size of the antenna.

Patch antennas in general can be classified in terms of the shape of the patch. The patch

can be square, rectangular, circular, elliptical, triangular, ring, sectoral ring or many more shapes. The rectangular patch is one of the most popular antennas and has been chosen for the design of the single element MPA in this thesis because a rectangular patch provides option to tune two sides. Thus, from designer's perspective one side can be used to vary resonance frequency while other side can be independently used to vary radiation pattern. Also, since only width of the patch gives rise to radiation there is less issue of unwanted cross polarization. A general figure of a R-MPA is presented below.

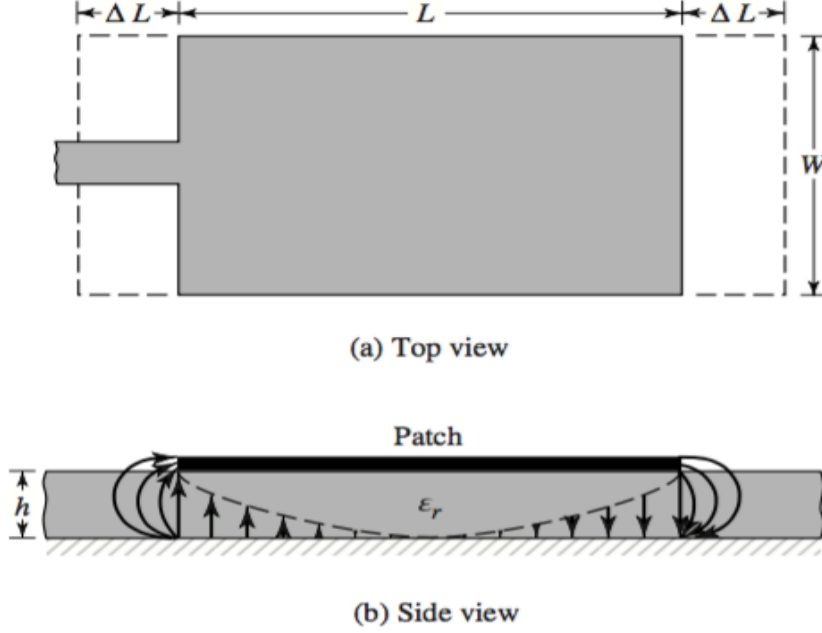


Fig. 3.1 Rectangular Microstrip Patch Antenna[8]

There are several ways of exciting a patch antenna, some of the most common being the coaxial probe, microstrip line, aperture coupling and proximity coupling. The aperture and proximity coupling techniques of feeding the antenna gives a significant increase in bandwidth but the fabrication process for them is very difficult compared to the coaxial and microstrip feeding techniques. Coaxial feeding is when a coaxial connector is used to

feed the antenna. Here, the inner conductor of the cable is connected to the patch through the connectors and the outer conductor is connected to the ground. This method of connection has narrow bandwidth and modeling becomes quite difficult above height (of substrate) of $0.02 \lambda_0$.

In the microstrip-feeding technique, a microstrip line of proper width serves as a transmission line between the source and the patch. Generally, the transmission line penetrates the patch towards the area where the patch has impedance of nearly 50 ohms for better impedance matching. The microstrip-feeding technique is the easiest in terms of modeling. However, with increase in height of the substrate, the spurious radiation as well as the surface wave increases, which limits the bandwidth of the antenna to about three percent of the targeted carrier frequency [8].

Microstrip feeding is also very convenient when it comes to fabricating an array of printed antennas. Designing antennas in arrays is well practiced in the field of wireless communication in order to enhance the performance of antenna parameters like directivity and gain. Array antennas also have the ability to steer the radiation beam by feeding signals of varying phase to individual elements of the array [12]. Terms related to an array antenna and its analysis are discussed in detail in section 4 of this thesis. For this thesis microstrip feeding technique is used because the microstrip line can later be used when designing array antenna. The microstrip feeding technique reduces complexities in designing impedance matched power dividers to serve the array antenna.

3.1 Modeling of Rectangular-Microstrip Antenna

In order to investigate a rectangular microstrip antenna in terms of its dimensions, impedance, efficiency and other parameters, several studies, mathematical modeling and interpretations have been carried out. Though multiple mathematical models have been presented by several researchers throughout time, the most common of them are the transmission line model and the cavity model.

3.1.1 Transmission Line Model

In the transmission line model, the R-MPA is evaluated as an analogy with a section of a transmission line. One of the early researcher to introduce this concept was Derneryd [13] in 1978. Throughout time, the same concept has been further refined by several antenna experts like H. Pues, A. Van de Capelle [14] and others. It is the easiest model of all but is considered the least accurate. But this model is very important as it gives deep insight into the R-MPA. Because a patch is an open- circuited transmission line with conductors on top and bottom, with no conductor at the sides, the electric fields within it cannot immediately vanish to zero at the edge. The electric fields instead exhibit fringing effects as shown in fig 3.2 (b).

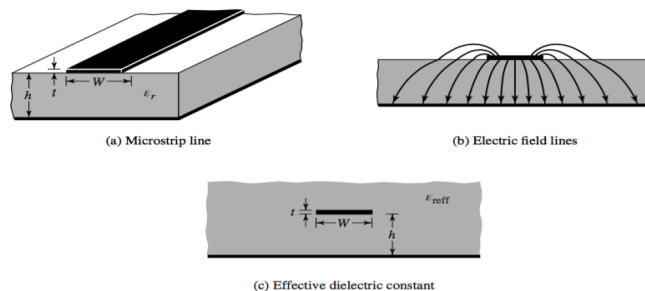


Fig. 3.2 Electric field lines in a microstrip line generating effective dielectric constant[8]

Now, as the E-field lines are travelling through the substrate as well as air, as in fig.3.3(b)

this confinement of E-field can be viewed as if there is a new substrate with new dielectric constant that takes care of both air and the original permittivity of the substrate, as shown in fig 3.3 (c). This new permittivity is called the effective dielectric constant (ϵ_{eff}). Let W be the width of the transmission line and h be the height of the transmission line above the ground plane, then as long as $W/h > 1$ the value of the effective dielectric constant is given by:

$$\epsilon_{\text{eff}} = \frac{\epsilon_r + 1}{2} + \frac{\epsilon_r - 1}{2} [1 + 12 \frac{h}{W}]^{-0.5} \dots (3.1)$$

Similarly,

$$\Delta L = h \times 0.412 \times \frac{(\epsilon_{\text{eff}} + 0.3)(\frac{W}{h} + 0.264)}{(\epsilon_{\text{eff}} - 0.258)(\frac{W}{h} + 0.8)} \dots (3.2)$$

which leads to

$$L_e = L + 2\Delta L \dots (3.3)$$

where L_e is the effective length that accounts for the fringing effect.

For the dominant TM_{010} mode, the resonant frequency of the microstrip antenna is a function of its length, which is expressed mathematically below

$$(f_r)_{010} = \frac{v_0}{2 \times L \times \sqrt{\epsilon}} \dots (3.3)$$

Likewise, C.A Balanis in [8] also reports the conductance and finally input impedance of the patch. The input impedance plays a vital role in design of any high frequency device. In a high frequency system, the input signal tends to reflect back to the source if it is exposed to change in impedance, thereby increasing the voltage standing wave ratio (VSWR). The amount of reflection is termed as reflection coefficient (Γ). Γ (defined in

section 2.5) is a function of impedance of the mediums where the signal is travelling to and from.

As reported in [8], the input impedance ‘ R_{in} ’ of a R-MPA is given by

$$R_{in} = 90 \frac{\epsilon_r^2}{\epsilon - 1} \left(\frac{L}{W} \right) \dots (3.4)$$

In order to minimize reflection of input power, the inset feed that transfers power from source to the patch is penetrated into the body of the patch around the region where the patch resistance decreases to nearly 50 ohms. As depicted in fig 3.3, the 50Ω resistive region can be found using the following equation:

$$R_{in}(y=y_0) = R_{in}(y=0) \left(\cos \left(\frac{\pi}{L} y_0 \right) y_0 \right)^2 \dots (3.5)$$

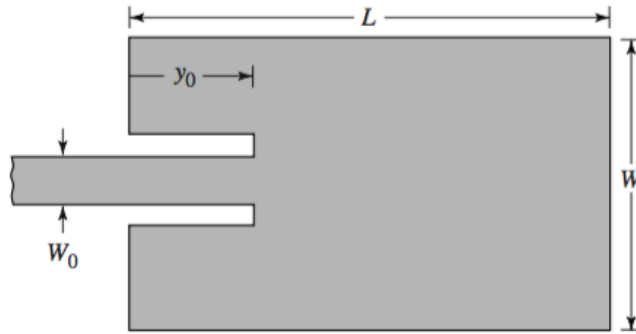


Fig. 3.3 Inset feed to 50Ω region of patch[8]

Though the mathematical expression for input impedance in terms of length ‘y’ has been presented above, it is common practice to determine this length using computer simulation software like CST and HFSS. Such simulation software, which is described in chapter 5 of this thesis, can be used to sweep the length of the inset and compare the VSWR the simulation provides in every sweep. In general practice, lower VSWR is better, however

VSWR less than 1.5 is considered in several research papers.

In this thesis the length and width of the rectangular MPA are calculated based on equations 3.1 and 3.2 and based on transmission line model defined in [8]. Similarly, the inset feed of the RMA where the path has input impedance of 50 ohms was calculated using equation 3.5. In this way the transmission line model was used for designing the rectangular MPA for this thesis.

3.1.2 Cavity Model

The R-MPA antenna can also be approximated as a cavity of dielectric which is bounded by conductors on top and bottom and also bounded by magnetic walls (to agree with the open circuit nature of section 3.1.1) along its perimeter. This approximation will certainly force the antenna to look reactive rather than real i.e. it doesn't radiate any power, which is not true. However, this approximation is useful as it gives better insight and prediction of computed patterns, input admittance and resonant frequencies.

As shown in fig. 3.4, when a path antenna is energized, a charge distribution is established on the upper and lower surface of the patch. This also forces the charges to be induced on the ground plane.

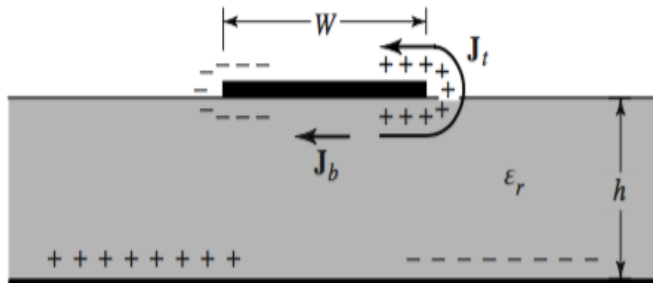


Fig. 3.4 Cavity model representation of R-MPA[8]

The attractive force between the unlike charges under the patch and the charge on the

ground plane forces the charge concentration on the bottom of the patch, resulting in current ' J_b '. Current ' J_t ' is produced as a result of repulsion between like charges above and below the patch. For almost all practical microstrips, the H/W ratio is small, which makes the attractive force dominant. This means most of the current in a microstrip flows under the patch.

The fringing fields also help us understand why a patch actually radiates. As the length of the patch is designed to be half the length of wavelength in the substrate, the electric field under the patch can be arranged in the manner shown in fig.3.5.

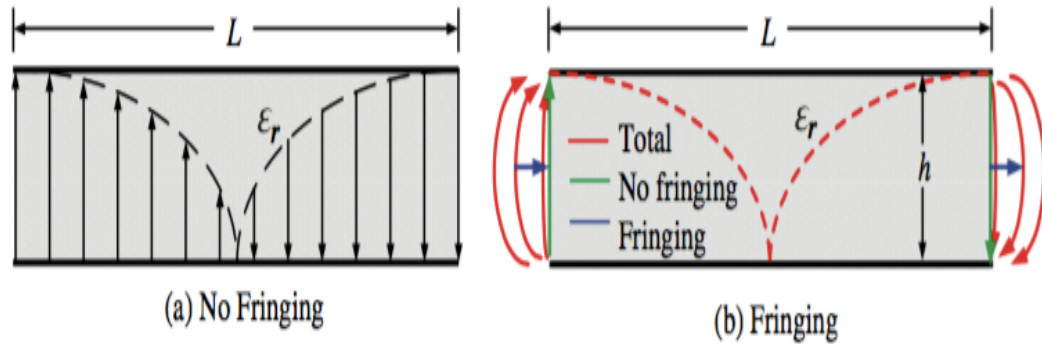


Fig. 3.5 Effect of fringing field in R-MPA[8]

As seen in fig.3.5, when the length of patch equals half-wavelength of the input signal inside the substrate, the electric field distribution should be such that it is zero in the center of the length and also maximum and opposite on the edges. But, since the perimeter of the patch is not surrounded by conducting walls, the E-field undergoes a fringing effect, also demonstrated in section 3.1.1.

It can be observed in figure 3.5 that these fringing fields on the sides are the only fields that have the horizontal field components in phase with one another. Thus for a time varying input signal, these fields will also reverse their polarity, giving rise to time varying electric fields. These time varying E-fields are in fact the true reason behind the radiation.

The definition of permittivity implies that with higher dielectric constant of the substrate, the electric fields within the substrate are more constrained, which also means that the bows of the fringing fields are also contained for substrate with higher ϵ_r . As the fringing fields are actually responsible for radiation, it can be concluded that efficiency of radiation decreases with substrate with higher permittivity.

Because printed circuit board (PCB) technology is mostly preferred for microstrip antenna locally and also because PCB technology is used for fabrication of the antenna for this thesis, the word “substrate” has also been referred to as “circuit board” in upcoming sections of this thesis. It has been previously reported in this section that defining a patch as a cavity surrounded by conductors on two sides and magnetic walls on perimeters will force the antenna to look reactive rather than real. In actuality the loss tangent of the substrate makes the circuit board acts as load resistance (R_L) and radiation resistance (R_r). The radiation resistance is our subject of interest which we wish to increase for more radiation.

Solving for the vector potential, using the homogeneous wave equation, electric and magnetic fields along x, y, and z axis have been reported in [16]. The lowest resonant mode at TM010 mode is:

$$(f_r)_{010} = \frac{v_0}{2 \times L \times \sqrt{\epsilon}} \dots (3.6)$$

while electric and magnetic components in several axes are given by:

$$E_x = E_0 \cos\left(\frac{\pi}{L}y'\right) \dots (3.7)$$

$$H_z = H_0 \sin\left(\frac{\pi}{L}y'\right) \dots (3.8)$$

$$E_y = E_z = H_x = H_y = 0 \dots (3.9)$$

4. ARRAY ANTENNA

An antenna array in general can deliver more features compared to a single element of the array. Arrays can be used to synthesize a required pattern that a single element may not provide. Arrays are well known for their attributes like scanning a beam, increasing directivity and gain. This chapter of thesis introduces general topics on array antennas and correlates the idea with an array of microstrip antennas.

Arranging individual elements in an array brings more degrees of freedom in terms of position. Thus, the geometrical configuration is the first thing that comes up while talking about an array. A linear array is one where all elements are in the same row. If the elements are distributed in a plane rather than a single dimension, then the geometrical orientation of the array is called a planar array. Rectangular and circular orientation are the best examples of a planar array. Non-planar arrays like cylindrical and spherical are also used in specific applications, for example space communication.

The second important thing in an array antenna after geometrical orientation is the relative placement of individual elements. The distance between individual elements plays a vital role in array performance as the elements collectively contribute to radiation and mutually couple one another. Generally, the spacing between elements is always a constant term while different spacing has also been studied and reported. As an example, in [15] the spacing between individual antennas has been swept to study improvements on reduction of side lobes.

The third thing to keep in mind while designing an array antenna is the excitation of discrete components in terms of amplitude and phase. Variation in amplitude and/or phase while exciting elements of an array is very handy for shaping and steering the beam. Scanning

radars that detect aerial vehicles use this technique to scan the space, identify and get basic information like distance and shape of an aerial vehicle.

For arrays where all elements are identical, there are two almost independent variables that control the radiation pattern of the array antenna. The first is called the radiation pattern of single element (also known as the element pattern), and the second is called the array factor. The array factor is the radiation pattern shown by the array if the elements were replaced by isotropic radiators. The total radiation pattern E (total) is given by following equation [16],

$$E \text{ (total)} = E \text{ (single element)} \times \text{Array Factor} \dots (4.1)$$

4.1 Linear Array Factor

For any array with all elements identical, if we note ‘d’ as spacing between elements and ‘ β ’ as the progressive phase difference between them, then the linear array factor is given below.

$$AF = \sum_{n=1}^N e^{+j(n-1)(kd \cos \theta + \beta)} \dots (4.2)$$

where “ θ ” is the angle made between the axis of the linear collection of antennas and the observation point in space where radiation characteristics are determined. Similarly, “n” is the number of elements in the array.

The term $kd \cos \theta + \beta$ is also collectively termed as relative phase (φ). Relative phase is then used to determine the progressive phase difference (β) between elements so that the beam can be directed in desired angles in space. Generally, computer controlled algorithms are used in association with phase shifters to achieve beam steering. Since beam steering

is not the center of focus for this thesis, further discussions on phase shifting and end-fires are limited.

4.2 Planar Array Factor

As mentioned earlier, when the elements on the array antenna are distributed in a plane rather than a particular direction, such an antenna system is called a planar array antenna.

Fig. 4.1 shows a diagram of rectangular planar array.

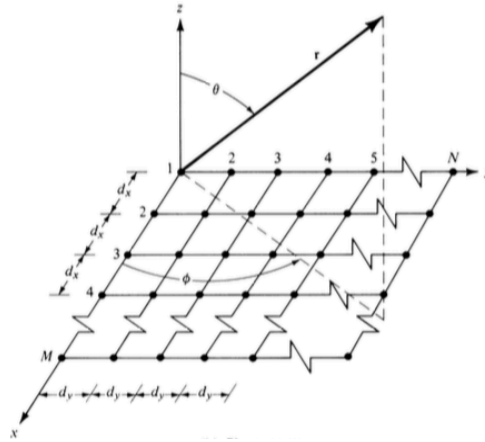


Fig. 4.1 Representation of planar array[8]

If “dx” and “dy” are the spatial separations between elements in X and Y directions as shown in fig. 4.1, then the array factor for such a system [16] of elements is mathematically represented by equation below.

$$AF(\theta, \phi) = A \times B \dots (4.3)$$

where

$$A = \frac{1}{M} \frac{\sin\left(\frac{M\phi x}{2}\right)}{\sin\left(\frac{\phi x}{2}\right)} \dots (4.4)$$

and

$$B = \frac{1}{N} \frac{\sin(\frac{N\varphi y}{2})}{\sin(\frac{\varphi y}{2})} \dots (4.5)$$

Here, “M” and “N” represent the number of column and row in the array as shown in fig.4.1.

Similarly,

$$\varphi x = kd_x \sin \theta \cos \phi + \beta \dots (4.6)$$

$$\varphi y = kd_y \sin \theta \sin \phi + \beta_y \dots (4.7)$$

where “k” is the wave number which is equal to $\frac{2\pi}{\lambda}$.

The above mentioned equation is then used to identify appropriate values of phase differences between adjacent elements for values of azimuthal angle “ ϕ ” and elevation angle “ θ ”, which will then identify radiation characteristics at any point in space surrounding this rectangular planar array antenna.

For this thesis a planar (rectangular) array has been studied. The above-mentioned mathematical models could be used as an alternative of simulation software for analyzing such an array. Fig.4.2 shows a picture of the rectangular array of four patches designed for this thesis.

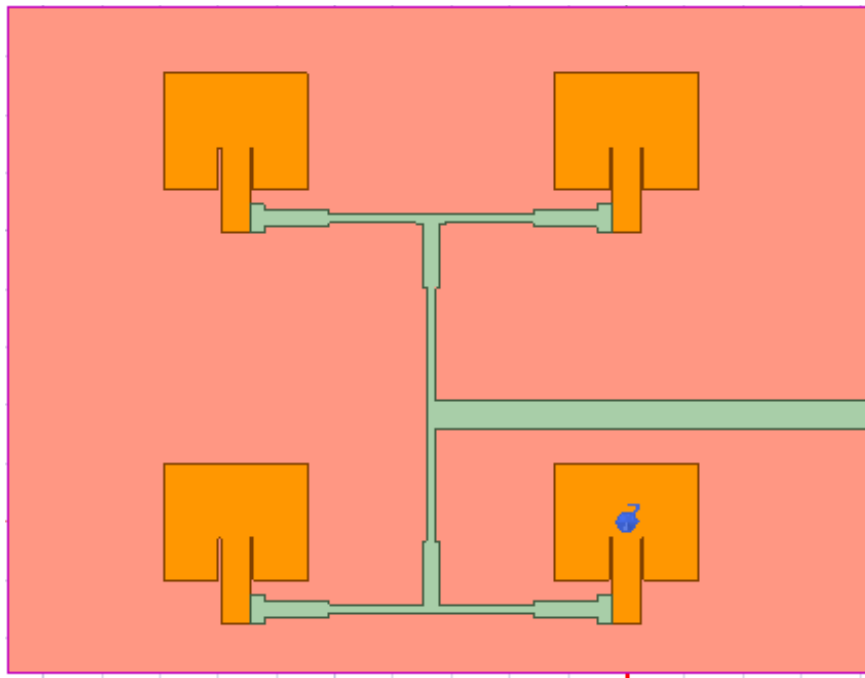


Fig. 4.2 Simulated rectangular array

Similar to rectangular arrays there are other common forms of planar arrays e.g. circular arrays. Since the rectangular array is the subject of interest for the thesis, further discussions on other forms of planar array are not considered in this thesis.

5. COMPUTER PROGRAM FOR SIMULATION OF HIGH FREQUENCY DEVICES

With increasing computational power, more and more designs of RF components like antennas, waveguides, transmission lines, filters etc. are first designed in computer aided software and then strategically studied. Such study mostly involves solving electromagnetic equations like the one proposed by Maxwell. Several companies have their own versions of such software and the exact mathematics and procedure they use may vary significantly. Some examples of such software are FDTD, CST, FEKO, COMSOL, MOMENTUM and XFDTD. In this thesis, HFSS is used for design and simulation of the R-MPA and its array. Thus, this chapter of the thesis discusses the basic concepts behind the HFSS and mathematics related to it.

The High Frequency Structure Simulator (HFSS) is one of the recognized simulation packages distributed by ANSYS Software Company. HFSS uses a mathematical technique called the Finite Element Method (FEM). In order to solve field equations using FEM, it uses a technique called the Adaptive Solution Process (ASP). In ASP, the three-dimensional structure of the design is first separated into a huge number of geometrically conformal meshed elements. The electromagnetic field existing inside every mesh is then solved in the solution frequency, based on the boundary condition. The equations involved are mentioned below. [17]

$$\nabla \times \left(\frac{1}{\mu r} \nabla \times \mathbf{E} \right) - k_0^2 \epsilon_r \mathbf{E} = 0 \dots (5.1)$$

which yields to

$$\nabla \times \left(\frac{1}{\mu r} \nabla \times \mathbf{E}^{\text{approx}} \right) - k_0^2 \epsilon_r \mathbf{E}^{\text{approx}} = \text{residue (or delta S)} \dots (5.2)$$

The above equation is iterated until a user-defined value of minimum error is meet. For every iteration, the tetrahedra with high residue values are selected and refined. The HFSS program starts with modeling a geometry and ends with post processing the result. In between there are four more steps. All six stages of HFSS simulation are introduced in described in general in the following sections of the thesis.

5.1 Create model/Geometry

All HFSS design starts with modelling the structure. For example, in order to study a waveguide via simulation in HFSS, the starting step is to provide dimensions and material properties of the waveguide. For every length, breadth and other geometrical properties of a discrete piece of a design, it is very practical to provide parametric values. In this way, the parameters can later be changed (or tuned) so that performance wise, the perfect design can be reached.

Alternative to using the above mentioned inbuilt 3D modeler in HFSS, users can also import 3D structures from other mechanical drawing packages like AutoCAD, SolidWorks etc. However such imported files lose their history and have to be manually altered in order to be parametrized.

5.2 Assign Boundary

The main purpose of the boundary is to create an open or closed electromagnetic model. A closed model is the solution volume where energy cannot leak except from the applied port. Some examples of this are the cavity resonator and waveguide. Similarly, an open model is where electromagnetic energy can radiate away. An antenna or a PCB can serve as an

example of this type. By default, HFSS treats background as a perfectly conductive boundary, or as a closed model. Therefore, if necessary, users have to define a boundary, generally called the radiation-boundary, to force the design to be an open model.

Another reason for applying a boundary is to simplify the complexity of the design. For example, it is easy to define the reflector of a dish antenna as a perfectly conducting boundary, rather than defining it as some metal with numerous characteristics. This will save considerable simulation time, requires less computational power and ends up giving almost the same results. Thus, meticulous understanding and selection of boundaries can be very helpful in HFSS, as they decide several aspects of simulations including time, complexity and accuracy.

5.3 Excitation in HFSS

All passive components must be excited with an external source in order to investigate their behavior. Depending on the nature of the design and interests of the user, HFSS provides seven options for exciting the device under investigation. Out of the seven, “wave port,” “lumped port” and “floquet port” yield results in the form of scattering-parameter (commonly called S-parameters). The remaining excitation modes, namely incident field, current source, voltage source and magnetic bias source, yields the final results in the form of field information.

Since wave ports and lumped ports are the most commonly used excitation methods and are also thoroughly used in this thesis, a quick introduction to these modes is collectively presented. The wave port and lumped ports can be used to generate field information as well as S, Y and Z parameters. In addition, the wave port also gives knowledge of wave

impedance and the propagation constant and propagation attenuation constant of a high frequency wave.

The HFSS calculates the 2D solution for the wave port first and then subsequently uses the solution as a source for the 3D solution. HFSS treats each solution as a wave port which is connected to a semi-infinite waveguide of the same exact cross section and material property as the port itself. These solution fields are then impressed onto the port region of the 3D model to obtain a solution to the 3D model [17].

5.4 Solution Frequency

Most of the parameters in electromagnetism, be they basic properties like permittivity, permeability and refractive index or their derivatives like S-parameters, reflection, transmission, and absorptions, are all functions of frequency, or in other words, wavelength. Thus, it is common sense that any high frequency simulator must have an option to select solution frequency (often called the targeted frequency of operation). This frequency will then allocate the size of tetrahedra mentioned in the introduction section of this chapter. Also, if a frequency sweep is desired for any simulation then the maximum frequency range for the sweep should be around 60 percent of the maximum frequency desired. If the solution frequency does not match the designs then the solution may not converge, resulting in incorrect results, which can be very misleading. Therefore, it is considered a very good practice to repeatedly look into the message box while the simulation is running to check if the solutions are converging. A warning box will appear if the solution doesn't converge at all in any number of adaptive passes.

5.5 The Delta S

In solving any higher order equation using computers, the user defines a number as the minimum error. The process for solving the equation is iterated in a loop, every time leading closer to the actual solution. This iteration terminates when the difference in the result reaches a value of minimum error defined beforehand. This minimum error in HFSS is called delta S, which leads us to the conclusion that a smaller delta S means longer simulation time and vice-versa. Generally, the value of delta S is defined between 0.005 and 0.01. It is up to the user to specify how close to the actual solution he/she wishes to reach. Sadly, the materials to be used for fabricating the real product cannot be 100 percent pure. This means if we specify a very small minimum error we may be wasting simulation time since the calculated solution is never perfect because of impurities in raw material in nature.

In case of HFSS the delta S is either the difference in S-parameters between consecutive passes or the difference in the electric field between successive solutions. This means that delta S is providing users the knowledge on how much the solution is converging which is then used to refine the tetrahedra for adaptive solution processes.

5.6 Post Processing

After the simulation is complete, the next thing the user wants to see is the result. S-parameter is the most basic data which is plotted at a single frequency or over a span of frequencies. The S-parameter generated is by default normalized to the impedance of the wave port designed, generally 50 ohms. So, if the port to be used in practice has a different impedance, re-normalization is necessary.

Similarly, advanced plotting of the result is also available in HFSS. Such processes are used to look into properties like Y-parameters, Z-parameters, VSWR, group delay, time domain reflectometry (TDR), gamma-parameters, etc.

In case of antenna simulations, it is also possible to view the far-field results as long as the radiation boundary is properly defined in the modeling section at the beginning. The far field result includes mostly real and realized gain, directivity, radiation characteristics etc. Another promising feature of HFSS is animation. Here the response of E and H fields can be animated on the designed structure over time. For example, in case of this thesis (or any patch antenna), it is possible to view surface current flowing under the patch. Such animation helps users to understand the nature, strength and role of such parameters which can be used for better understanding of the device and optimization of such devices.

6. DESIGN AND SIMULATION OF SINGLE ELEMENT RECTANGULAR PATCH ANTENNA

Several substrates were studied for the purpose of this thesis, which is designing a microstrip antenna for systems supporting Wi-Fi. As mentioned in previous chapters, the dielectric material of the substrate has direct implications on size and performance of the antenna. In the early research phase of the thesis, FR-4 substrate, which has dielectric constant of nearly 4.4 was considered. Several thickness of this substrate like 1.5 mm, 1.6 mm and 2 mm were studied. Because of their higher permittivity which results in low gain of antenna and their unreliability in terms of purity, this substrate was finally taken out of consideration. Meanwhile, several other substrates were also comparatively studied. From them, finally Roger's RT_Duroid 5880 was selected because the substrate has lower relative permittivity, is commercially available and has better reliability in terms of material purity.

It has been recorded and also noticed during the thesis that the bandwidth of the printed antenna, excited by transmission line, under normal circumstances, can reach close to 3 percent of targeted frequencies. In our case, we were targeting for at least 2.4 GHz to 2.47 GHz so that it can be reliably used for Wi-Fi, IEEE 802.11 standards. The design started by selecting the height of the patch from the ground plane to be 1 mm. It should also be noted that the thicker the substrate, the wider the bandwidth it supports. This is because now the antenna is utilizing the volume around it more efficiently. To correlate this idea, an increase in bandwidth can also be noticed in a dipole antenna. Increasing the thickness of the poles while keeping all other parameters unchanged increases the bandwidth of the dipole.

It has been mentioned in chapter 3 that the height of substrate can range from $0.003 \lambda_0 \leq$

$h \leq 0.05 \lambda_0$.

For our case:

Frequency in free space (f_0) = 2.4 GHz $\rightarrow \lambda_0 = 124.9$ mm

thinnest substrate = $0.003 \lambda_0 = 0.37$ mm

thickest substrate = $0.05 \lambda_0 = 6.245$ mm

After investigating material availability in the local market, and to avoid any potential time lag due to material lead time, finally RT_Duroid 5880 of thickness 3.175 mm was used.

The HFSS design of the top view of the patch antenna is shown below in Fig. 6.1.

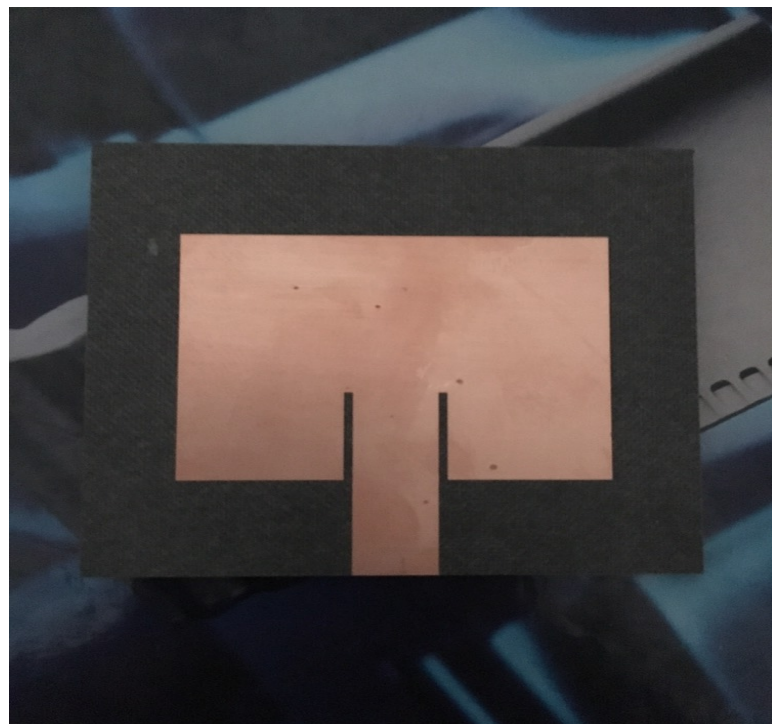


Fig. 6.1 Top view of R-MPA

In the above picture, the brown (copper) portion shows the conducting patch and the transmission line. Similarly, the black portion represent the substrate or the PCB board. The PCB board has 1 oz. copper layer deposited on both sides. Thus, the patch and

transmission line were protected and remaining portions of copper were etched off during fabrication. The copper on other side of the substrate was not disturbed as it serves as a conducting ground plane. Comparing fig.6.1 with fig. 3.4, the values for L, W, y_0 and w_0 are respectively 39.88 mm, 49.26 mm, 13.68 mm and 9.87 mm.

Similarly, the two narrow insertion gaps between the patch and the transmission lines have width of 1mm.

The value for ‘L’ and ‘ y_0 ’ were selected based on equations provided in chapter 3. These values were then carefully tuned in HFSS, until optimized value in terms of S11 was gained. The thickness of the transmission line was calculated based on equation (6.1) mentioned below. The thickness was selected to be at 50 ohms, so that locally available connectors and spectrum analyzers can then be used with minimal energy stranded as standing waves.

If $W/d > 1$; d being the height of transmission line from ground (thickness of PCB board), we have impedance (Z_0) of the transmission line given by:

$$Z_0 = \frac{120\pi}{\sqrt{\epsilon_r} \left[\frac{w}{d} + 1.393 + \frac{2}{3} \ln \left(\frac{w}{d} + 1.444 \right) \right]} \dots (6.1)$$

After finishing all necessary designs, assigning elemental properties and defining frequency sweeps in HFSS, simulation was carried out. After simulating the design using HFSS, several results were obtained which are shown in following sections.

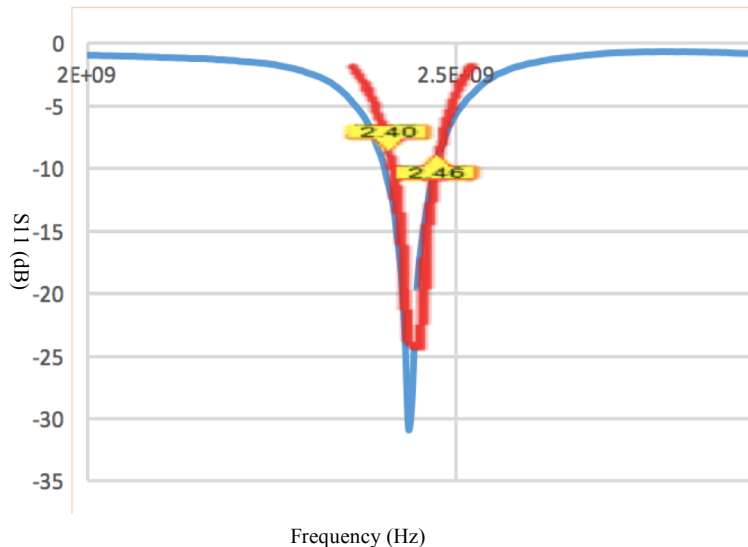


Fig. 6.2 Simulated (red) and measured (blue) S11

In fig.6.2 it can be observed that the simulated reflection coefficient of the antenna (shown in red line) crosses -10 dB at 2.40 GHz all the way up to 2.46 GHz. This indicates that the antenna resonates well in these frequencies and has a bandwidth of 0.06 GHz (2.46-2.40) or 60 MHz.

Similarly, measuring the same antenna using a Vector Network Analyzer (VNA) it can be observed that the antenna has measured return loss (shown in blue line) below -10 dB from 2.4 GHz to 2.7 GHz. Comparing red and blue lines in fig.6.2 we can conclude the expected S11 from simulation and the measured S11 from the fabricated antenna are in very close agreement.

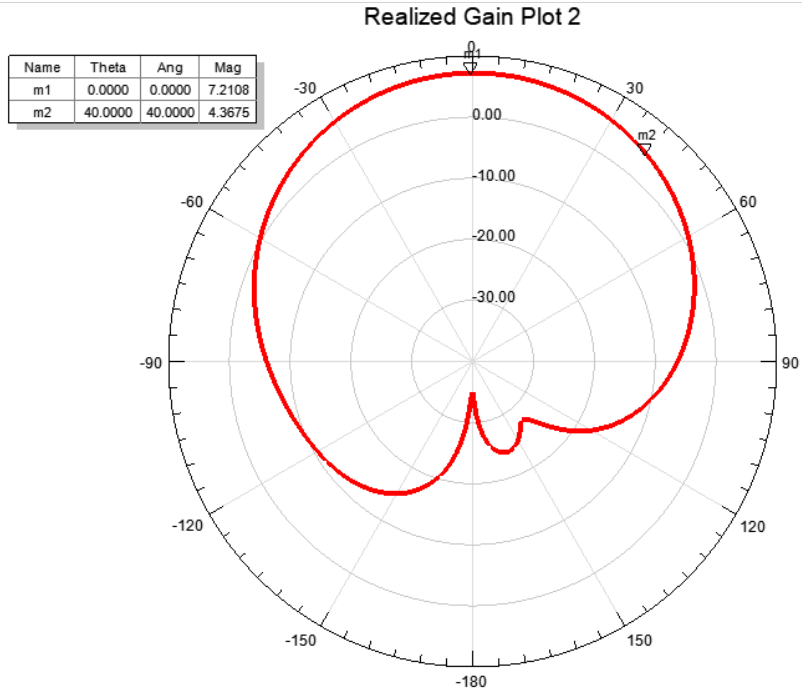


Fig. 6.3 Polar plot of realized gain in 2-D

Another promising feature that can be used to understand the true nature of an antenna is its radiation pattern. Fig.6.3 shows the simulated two-dimensional realized gain of the single element rectangular microstrip antenna in logarithmic scale. The above plot is a polar plot of realized gain vs azimuthal angle (ϕ). From this figure it can be noticed that maximum gain is achieved in zero-degree azimuthal angle and has value of 7.2108 dB. This also means that the antenna has boresight facing perpendicular to the antenna axis. Also mentioned in section 2.2, the HPBW is another feature that can be abstracted from a radiation pattern of an antenna. The HPBW gives an idea of how wide the radiation of antenna is covering the space around it. It is defined as the difference in azimuthal angle where the gain is decreased to half (i.e. -3 dB) from its maximum value. From fig. 6.3, it can be observed that at 40° the value of realized gain falls to 4.3675 dB, which is almost 3 dB down from the maximum value of 7.21 dB. The same phenomenon is also observed in

the other half of the radiation pattern. From the above statements, it can be maintained that this antenna has a HPBW of nearly 80^0 in E-plane.

Similar to a 2-D polar plot, a 3-D polar plot can be used to better grasp the nature of radiation of the antenna. Figure 6.4 below represents the simulated 3-D polar plot of directivity of the antenna.

Directivity Plot 1

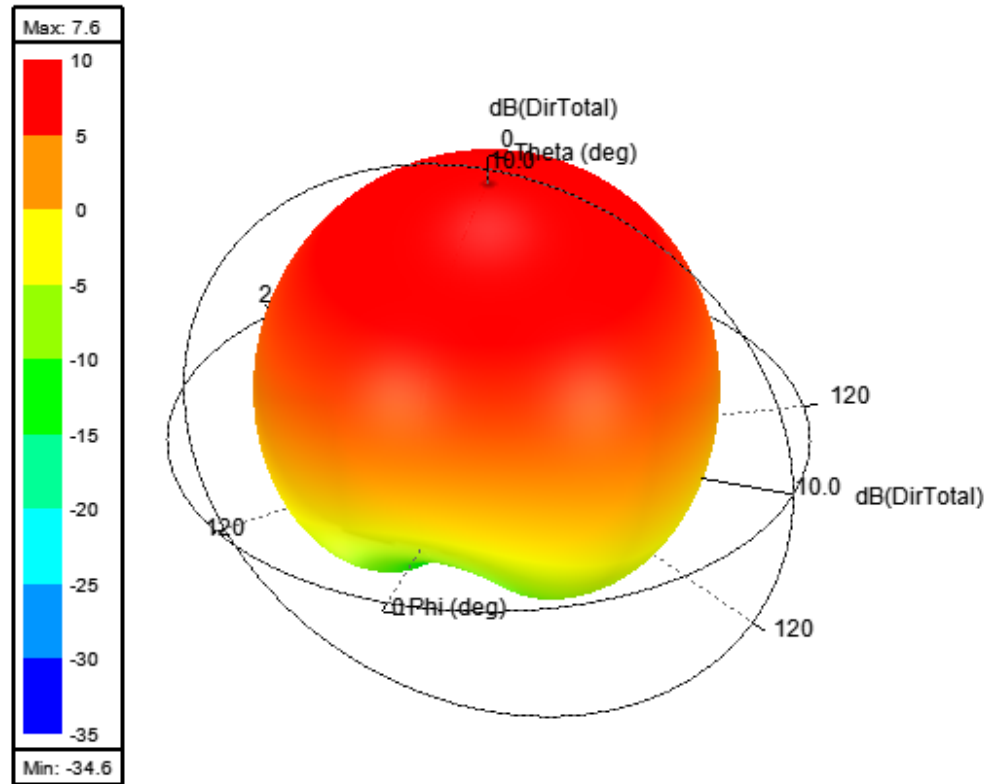


Fig. 6.4 Polar plot of directivity of R-MPA in 3-D

In this figure it can be seen that the R-MPA is radiating in the shape of a dome. Its major lobe, where most of its energy is confined, is represented by red pixels. Significantly, a

minor amount of energy can be seen around and below the axis where the antenna was aligned. These forms of energy are represented in fig 6.4 by yellow and green pixels.

Chapter 2 also discusses the efficiency of an antenna, which is the difference between the directivity and the gain in logarithmic scale. From figure 6.3 and 6.4, it can be observed that there is a difference of 0.39 dB, i.e. the designed antenna has an efficiency of 91 percent.

In section 3.1.2, it was mentioned that the current flowing below the patch due to attraction between unlike charges was the most dominating current. Thus, it is also equally interesting to visualize this current. This visualization of current gives better understanding of the physics involved and also works as the best starting point for future optimization. Fig.6.5 shows the surface current.

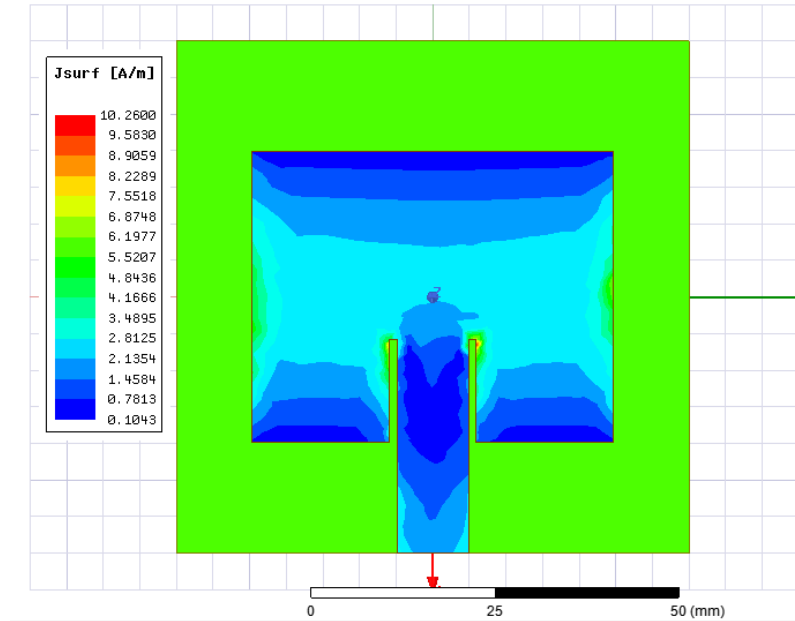


Fig. 6.5 Surface current gradient under the patch

The current under the patch represented by green pixels has maximum magnitude around 6 A/m. This signifies that the most current flows in the center of the edges of the patch. This is also the region where the voltage is zero because the patch has a length of half a wavelength. Study of changes of antenna parameters by altering shape and adding apertures in these significant regions of the patch can be an immediate topic for optimization in future projects.

7. FOUR ELEMENT ARRAY OF RECTANGULAR MICROSTRIP PATCH

After successful design of a single element patch, we move to our main objective for this thesis, which is design of a four-element array of the same single patch. For this purpose, a transmission line that works as a power splitter has been designed. Quarter-wave impedance matching of transmission lines has been used in order to connect the antenna with the splitter's network and then finally the terminal to this network of transmission can be connected to any practical device for operating the antenna. The transmission line design is shown in Fig. 7.1.

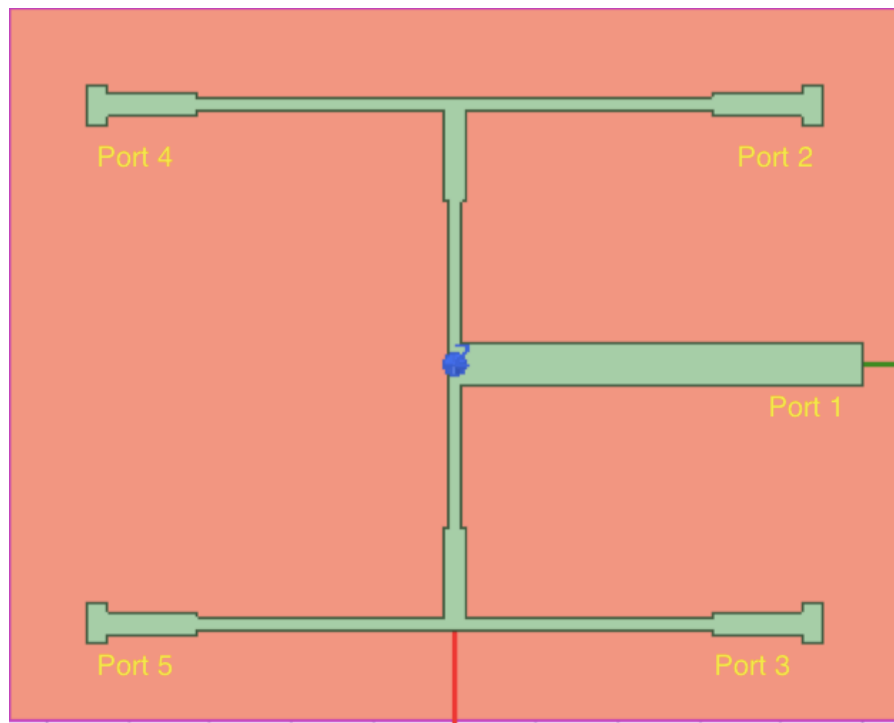


Fig. 7.1 '4×1' Power splitter using microstrip line

It can be seen in fig 7.1 that the transmission line starting from 50Ω (Port 1), is connect to two parallel lines of 100Ω . Each of these 100Ω lines is then matched to another 100Ω

parallel line by a quarter wave impedance transformer of 70.71Ω . These 100Ω transmission lines then connect to ports 2,3,4 and 5. This power splitter was then simulated separately to calculate its power splitting performance. The performance of this splitter in terms of reflection and transmission coefficients is represented in fig.7.2.

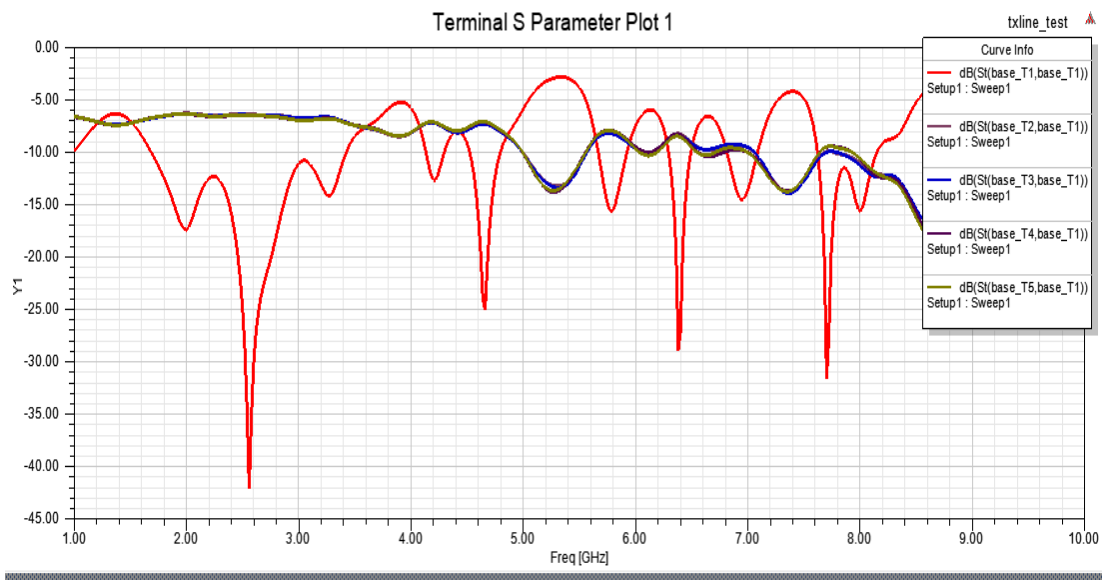


Fig. 7.2 S11, S21, S31, S41 and S51 of the '4×1' power splitter

In this figure it can be seen that the power transferred from port 1 is received by ports 2, 3, 4 and 5. The amount of power received by ports 2 to 5 is almost -6 dB, which means nearly 25 percent of power is received by each port. This is very logical and serves as a proof that the transmission line is properly designed as a 4×1 power splitter. The S11, also called the reflection coefficient, for this splitter around 2.4 GHz is deep to -40 dB and has a wide bandwidth. This knowledge of S11 guarantees that a very minimal amount of energy, at least around 2.4 GHz, is actually reflected back to the input port 1 and the splitter designed is performing very well.

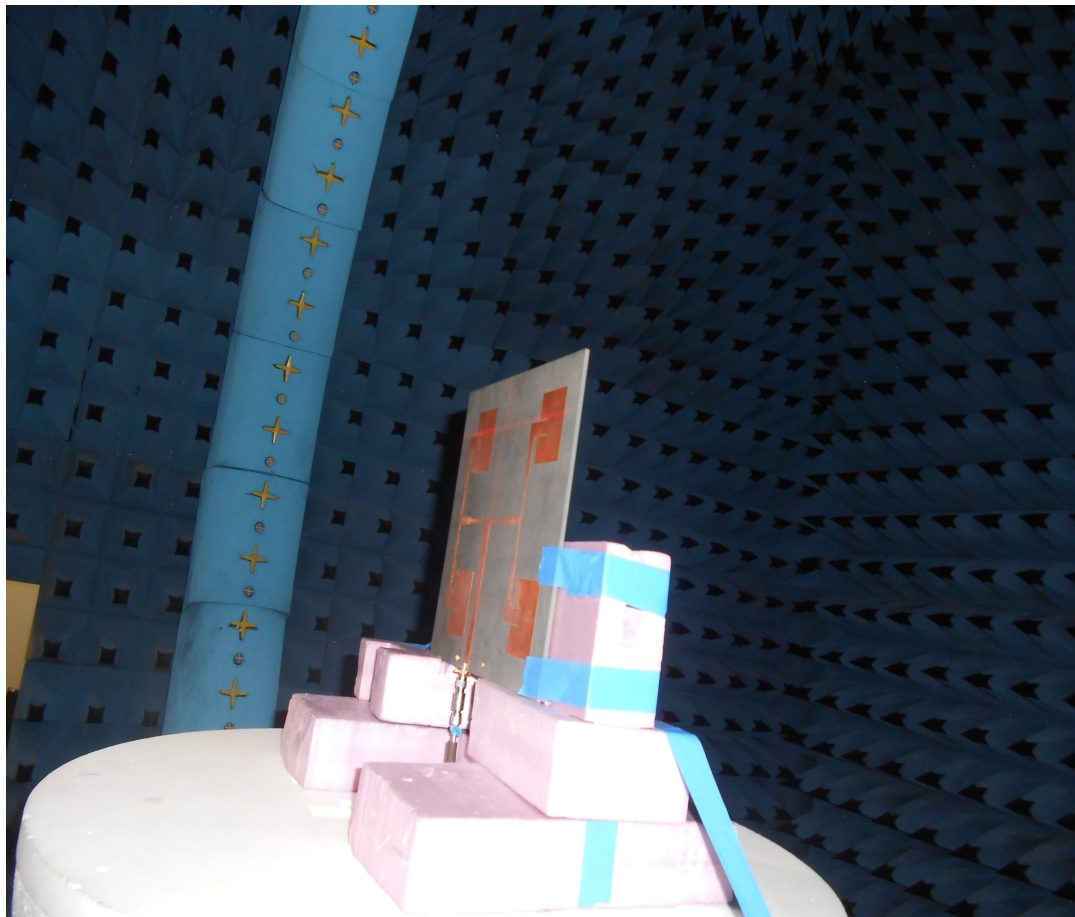


Fig. 7.3 Array antenna being measured in anechoic chamber

Fig. 7.3 shows the fabricated antenna being measured in an anechoic chamber. An anechoic chamber is a Faraday cage which is filled with pyramidal shaped RF absorbers from the inside. The absorbers are shaped in such a way that they have nearly 377Ω impedance. Since, this impedance is very close to the impedance of free space nearly all RF waves striking them get absorbed, thereby avoiding unwanted reflections. The Faraday cage shields the inner area from any electric signals from outside. In this way an anechoic chamber can be used to create an undisturbed environment for far-field measurement of any antenna.

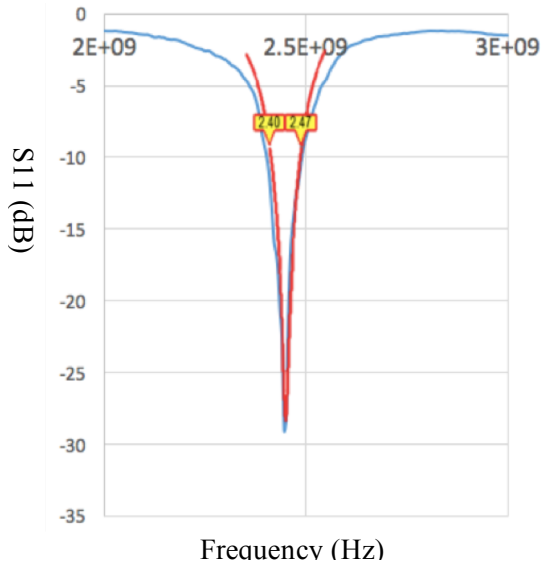


Fig. 7.4 Simulated (red) and measured (blue) S11

It can be seen in fig 7.4 that the simulated value of S11 (shown in red line) is in fact below -10 dB for frequencies ranging from 2.40 GHz to 2.47 GHz. This implies that the four element array is properly designed. The designed array has a bandwidth of 0.07 GHz (or 70 MHz). This frequency span in terms of percentage bandwidth is 2.91%. This also supports the fact that the microstrip feed line can provide bandwidth close to 3% as mentioned in chapter 3.

Fig 7.4 also shows the graph of the measured reflection coefficient (shown in blue line) in dB vs the frequency in Hz using a VNA. It can be seen that the array antenna has measured return loss less than -10 dB from 2.4 GHz up to 2.47 GHz which is in very close agreement to the simulated data shown in red line. Comparing the red and blue lines of fig.7.4 it can be concluded that the array antenna designed was indeed successful.

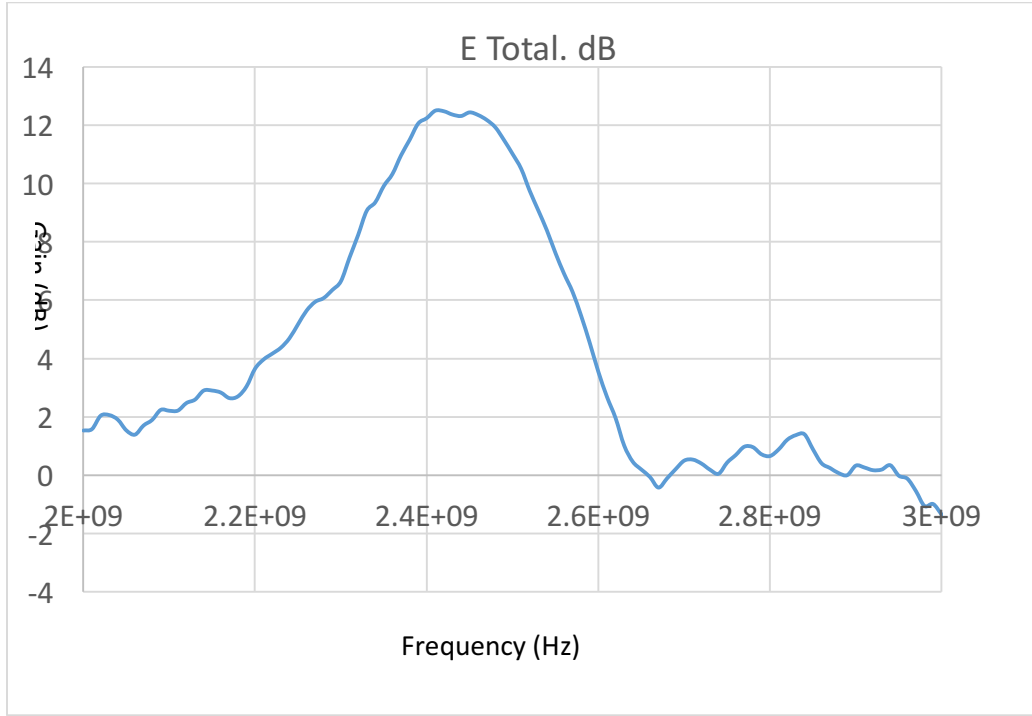


Fig. 7.5 Gain vs frequency plot

Fig 7.5 shows a plot of the measured gain of the array antenna in dB vs the frequency of the antenna in Hz. The graph clearly shows that the antenna has gain of 12.25 dB at 2.4 GHz. Similarly, it shows maximum gain of 12.50 at 2.41GHz. Starting from maximum gain at point 2.41GHz, the gain of the antenna reduces by approximately -3db at two points (2.35 GHz with gain 9.92 dB and 2.51 GHz with gain 10.51 dB). This 3 dB reduction in gain has a bandwidth of 0.16 GHz (or 160 MHz). This is the gain-bandwidth of the antenna.

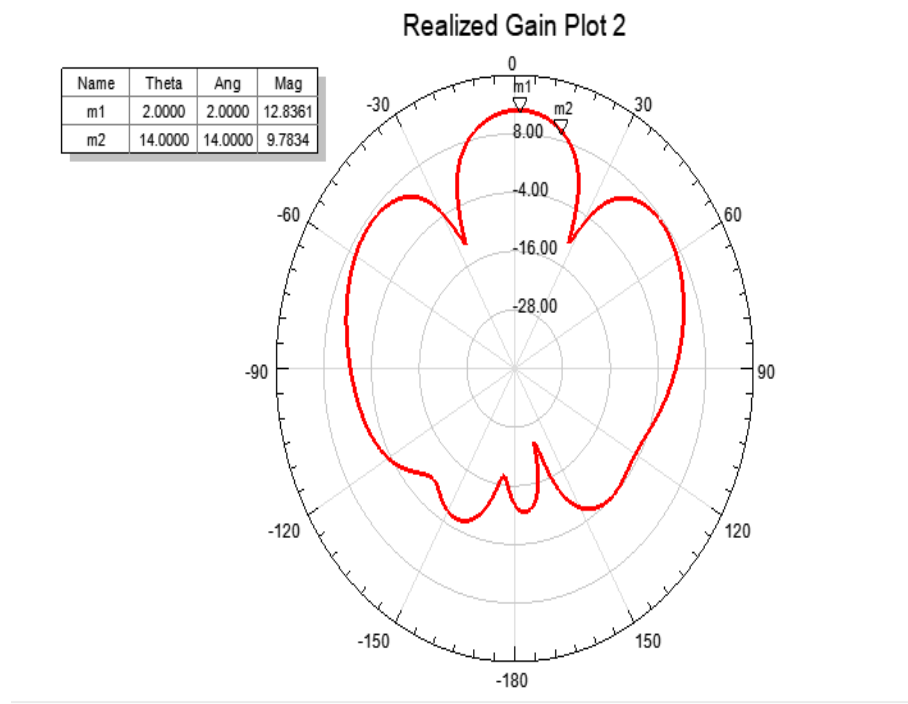


Fig. 7.6 Simulated 2-D plot of realized gain of the array antenna

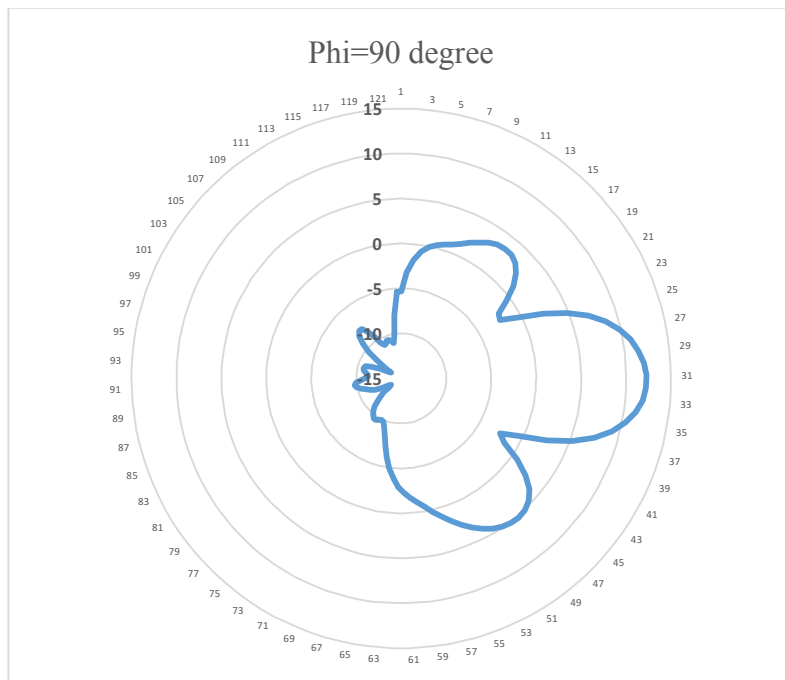


Fig. 7.7 Measured 2-D plot of realized gain in dB of the array antenna

Fig 7.6 and fig.7.7 show the 2-dimensional plot of simulated and measured realized gain

of the array antenna at 2.4 GHz respectively. From fig. 7.6 it can be observed that the maximum gain simulated was 12.8 dB which is in close agreement with the measured gain of the antenna in fig. 7.7 (and also fig. 7.5), which is 12.25 dB. Similarly, fig 7.8 shows the 3D plot of simulated directivity at 2.4 GHz and fig 7.9 shows the 2D plot of the measured directivity at different frequencies.

As mentioned in section 2.5, the efficiency of an antenna can be measured with the knowledge of the gain and the directivity of the antenna. At 2.4 GHz, the simulated gain of the array antenna (fig. 7.6) was 12.8 dB while the simulated directivity (fig. 7.8) was 13.5 dB. Thus, the simulated efficiency for the array antenna was calculated to be 0.7 dB (or 85 %). Similarly, the measured array antenna efficiency at 2.4 GHz is 80% which is shown in fig 7.10.

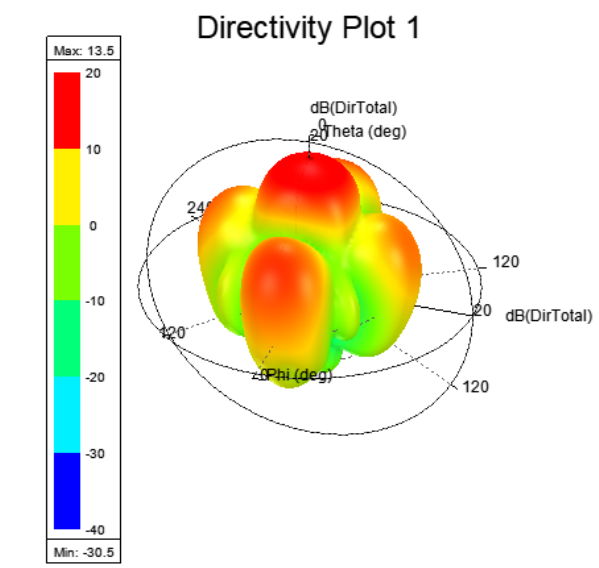


Fig. 7.8 Simulated Directivity of the array antenna in 3D

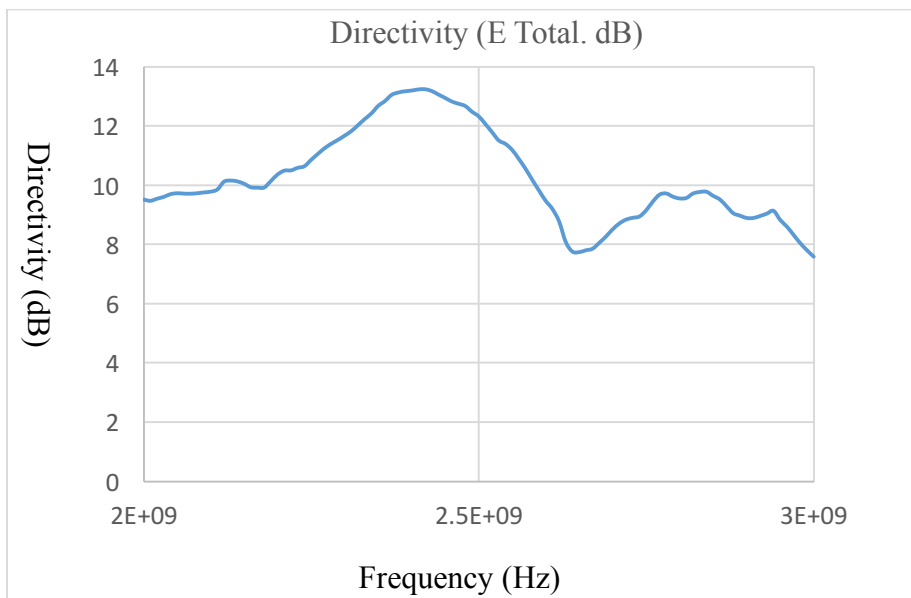


Fig. 7.9 Measured directivity of the array antenna (2D)

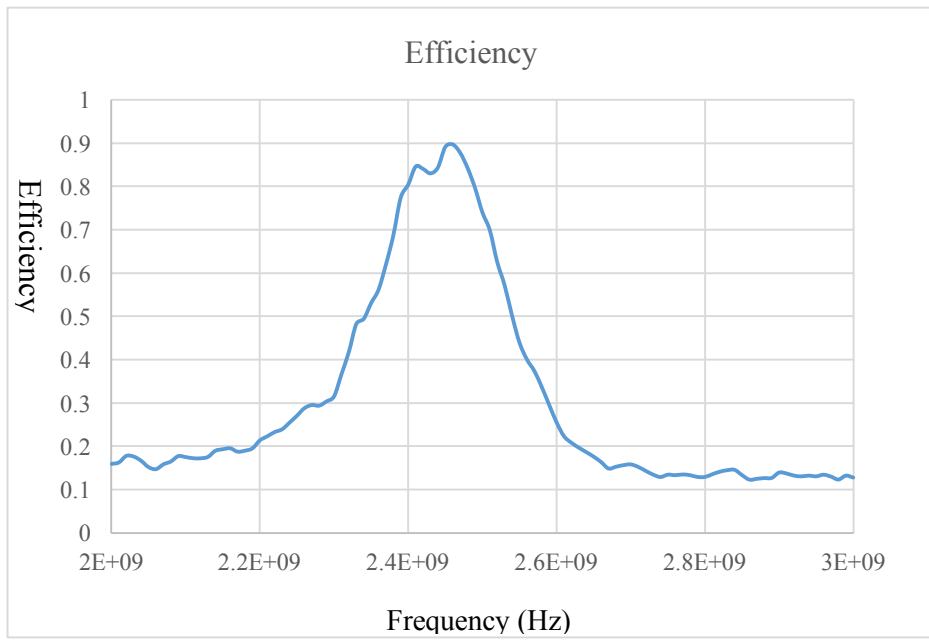


Fig. 7.10 Measured efficiency of the array antenna

8. DISCUSSION, CONCLUSION AND SUGGESTION FOR FUTURE RESEARCH

8.1 Discussion and Conclusion

In this thesis, we developed and analyzed an antenna that can support IEEE 802.11 at 2.4 GHz. The rectangular microstrip patch antenna (R-MPA) was selected for this purpose. The antenna was designed based on several equations shown in chapter 3. The ANSYS HFSS software package was used for designing the architecture of the antenna. This design was then simulated using the same software to estimate antenna parameters like directivity, gain, efficiency, radiation pattern and reflection coefficient.

The physical dimensions of the designed antenna were then tuned and the effect of tuning the dimensions on several antenna parameters like HPBW, bandwidth and gain were observed. Based on the requirement that the antenna should support the IEEE 802.11 at 2.4 GHz standards, the tuning of dimensions of the antenna was optimized.

The designed rectangular microstrip antenna was then used to create an array antenna with four elements. The purpose of implementing the array of the initially designed R-MPA was to study the enhancement of antenna parameters like directivity, gain and bandwidth with respect to the antenna parameters of the single element itself. For implementing the array of the single element antennas, a transmission line that serves as a 4×1 power splitter was designed and simulated using HFSS. The design of the power splitter involved a study of width of transmission line and quarter wavelength impedance matching. The reflection and transmission coefficients of the finally designed transmission line were then used to verify its quality. After successful design of the transmission line the four single element R-MPA

were attached to the ports of the power splitter. The distance between the single elements was then studied to reach better reflection coefficient. The whole structure, now called the “Four Element Microstrip Patch Antenna,” was simulated using the HFSS. The distances between the individual elements were tuned until optimized values in terms of antenna bandwidth and gain were reached.

The final optimized design of the four element MPA was then fabricated on a PCB board made of Rogers’ RT_Duroid 5880 material. This material has the dielectric constant of 2.2. The fabricated product is shown in fig.8.1.

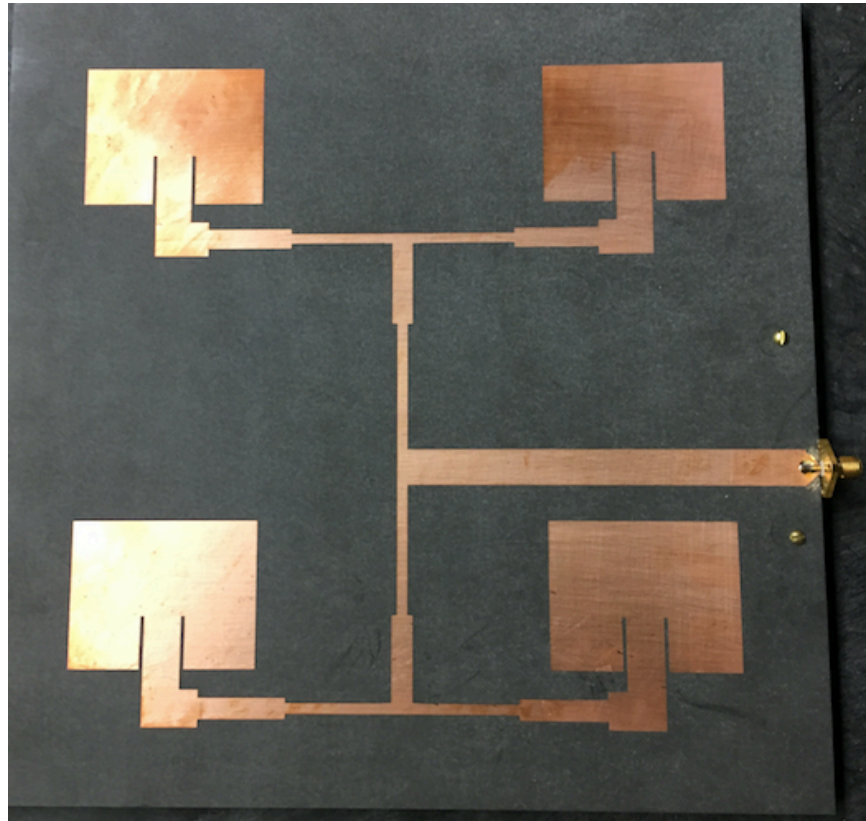


Fig. 8.1 Four element array antenna (220 mm × 225 mm board size)

The antenna was then connected with a SMA connector in order to connect it with test

setups like a Vector Network Analyzer (VNA) or a spectrum analyzer. The array antenna was then characterized in an anechoic chamber. The measured characteristics of the array antenna like gain, bandwidth, efficiency and radiation pattern were in good agreement with their corresponding simulated values. Thus, a successful study, design, fabrication and characterization of single element R-MPA and four element array of the initially designed R-MPA was carried out.

The array antenna was designed at 2.4 GHz and in order for it to accommodate 802.11b protocol it should have bandwidth of at least 72 MHz so that three non-overlapping channels in terms of frequency defined in the IEEE 802.11b protocol can be covered. The measured antenna has only 70 MHz bandwidth and is short on this aspect by 2 MHz. A summary of targeted, simulated and measured antenna parameters are listed in table 8.1.

Table 8.1 Summary of targeted, simulated and measured antenna parameters

Antenna Parameters	Targeted	Simulated	Measured
Frequency (GHz)	2.4	2.4	2.4
Bandwidth (MHz)	72	Single: 60	Array: 70
		Array: 70	
Gain (dB)	Single: 6-9	Single: 7.21	Array: 12.25
	Array: 8-13	Array: 12.83	
Efficiency	Single: 0.8-0.95	Single: 0.91	Array: 0.8
	Array: 0.8-0.95	Array: 0.85	

8.2 Suggestion for Future Research

8.2.1 Single Element R-MPA

For a microstrip antenna it is better to have smaller dielectric constant of the substrate, but for a microstrip transmission line substrates with higher value of dielectric constant are preferred. Thus, for future research it would be interesting to study designs with different substrate materials for the transmission line and radiating part of the antenna.

The microstrip antenna has very small bandwidth. There are ways where apertures can be introduced on the patch and/or on the ground plane of the microstrip antenna [18]. The collective effect of the microstrip patch and the aperture can then be used to enhance the bandwidth of the antenna. The same technique of introducing apertures of different shape and size on the antenna can be used to make the antenna radiate at multiple frequencies [19].

The concept of “fractals” where repeated patterns are either etched off or added on the original design can also be implemented on the single element antenna. Such techniques are known for improving antenna characteristics like gain and bandwidth [8].

8.2.2 Transmission line

An ordinary wire radiates even if a direct current passes through it if the wire is bent. The same radiation is also seen in transmission lines. So in future research, whenever transmission lines need to be bent to 90 degrees, at least one side of the transmission line can be trimmed at 45 degree angle to reduce reflections at the corners of the transmission line itself. This can increase the performance of the line by some amount. Similarly, instead of feeding the antenna with a coaxial transmission line, striplines and coupling technique can be used. Though comparatively more expensive than the transmission line technique, the coupling technique of feeding a microstrip antenna is known for improving the bandwidth [8].

I recommend to a future researcher designing the transmission line based on Wilkinson’s power divider technique [20]. This introduced resistors with mathematically calculated values of resistance between the branches of the transmission line. These resistors will dissipate any reflected signals which are more likely to be out of phase with one another. Because the reflecting waves from different ports are out of phase they will create a potential difference between branches of the transmission lines. Since these branches are now connected through resistors, the signals will then dissipate while traveling between the branches. This way the reflecting signals can be filtered out from mixing back to the source port and the performance of the transmission line can be improved.

REFERENCES

- [1] G. Kizer, Digital microwave communication: engineering point-to-point microwave systems. John Wiley & Sons, 2013.
- [2] G. A. Deschamps, "Microstrip microwave antennas," in Proceedings of the Third Symposium on the USAF Antenna Research and Development Program, Oct, 1953, pp. 18-22.
- [3] H. Gutton and G. J. F. p. Baissinot, "Flat aerial for ultra high frequencies," vol. 703113, 1955.
- [4] M. Gast, 802.11 wireless networks: the definitive guide. " O'Reilly Media, Inc.", 2005.
- [5] National Instruments. Introduction to Wireless Lan Measurements from 802.11a to 802.11ac," National Instruments. Available: <http://www.ni.com/rf-academy/>
- [6] R. G. Winch, Telecommunication Transmission system. The MacGraw-hill Companies, Inc, 1993.
- [7] International Telecommunication Union. Radio-frequency channel arrangements for fixed service systems. Available: https://www.itu.int/dms_pubrec/itu-r/rec/f/R-REC-F.746-5-200105-S!!MSW-E.doc
- [8] C. A. Balanis, Antenna theory: analysis and design. John wiley & sons, 2016.
- [9] K. Stephan, Analog and mixed-signal electronics. John Wiley & Sons, 2015.
- [10] M. F. Iskander, Electromagnetic fields and waves. Prentice Hall Upper Saddle River, 1992.
- [11] H. W. Silver, Ed. The ARRL Antenna Book for Radio Communication, 22 ed. The national Association for Amateur Radio Newington, 2011.
- [12] M. Bashri, T. Arslan, and W. Zhou, "A dual-band linear phased array antenna for wifi and lte mobile applications," in 2015 Loughborough Antennas & Propagation Conference (LAPC), 2015, pp. 1-5: IEEE.
- [13] A. J. I. T. o. A. Derneryd and Propagation, "A theoretical investigation of the rectangular microstrip antenna element," vol. 26, no. 4, pp. 532-535, 1978.
- [14] H. Pues and A. Van de Capelle, "Accurate transmission-line model for the rectangular microstrip antenna," in IEE Proceedings H (Microwaves, Optics and Antennas), 1984, vol. 131, no. 6, pp. 334-340: IET.

- [15] N. Ullah, Z. Huiling, T. Rahim, S. ur Rahman, and M. MuhammadKamal, "Reduced side lobe level of sparse linear antenna array by optimized spacing and excitation amplitude using particle swarm optimization," in 2017 7th IEEE International Symposium on Microwave, Antenna, Propagation, and EMC Technologies (MAPE), 2017, pp. 96-99: IEEE.
- [16] A. Z. Elsherbeni, C. Reddy, and P. Nayeri, Antenna analysis and design using feko electromagnetic simulation software (aces series on computational electromagnetics and engineering). SciTech Publishing, 2014.
- [17] M. J. A. Kopp, Pittsburgh, PA,, "An Introduction to HFSS: Fundamental Principles, Concepts, and Use," vol. 77, 2009.
- [18] A. A. Deshmukh, K. J. I. a. Ray, and w. p. letters, "Compact broadband slotted rectangular microstrip antenna," vol. 8, pp. 1410-1413, 2009.
- [19] A. Sarma, K. Sarmah, and K. K. Sarma, "Low return loss slotted rectangular microstrip patch antenna at 2.4 GHz," in 2015 2nd International Conference on Signal Processing and Integrated Networks (SPIN), 2015, pp. 35-39: IEEE.
- [20] K. Srisathit, P. Jadpum, and W. Surakampontorn, "Miniature Wilkinson divider and hybrid, coupler with harmonic suppression, using T-shaped transmission line," in 2007 Asia-Pacific Microwave Conference, 2007, pp. 1-4: IEEE.